Drug Design, Development and Therapy

Dovepress
open access to scientific and medical research

Open Access Full Text Article

ORIGINAL RESEARCH

Plumbagin induces G_2/M arrest, apoptosis, and autophagy via p38 MAPK- and PI3K/Akt/mTOR-mediated pathways in human tongue squamous cell carcinoma cells

This article was published in the following Dove Press journal:
Drug Design, Development and Therapy
16 March 2015
Number of times this article has been viewed

Shu-Ting Pan,[1] Yiru Qin,[2] Zhi-Wei Zhou,[2,3] Zhi-Xu He,[3] Xueji Zhang,[4] Tianxin Yang,[5] Yin-Xue Yang,[6] Dong Wang,[7] Jia-Xuan Qiu,[1] Shu-Feng Zhou[2]

[1]Department of Oral and Maxillofacial Surgery, The First Affiliated Hospital of Nanchang University, Nanchang, Jiangxi, People's Republic of China; [2]Department of Pharmaceutical Sciences, College of Pharmacy, University of South Florida, Tampa, FL, USA; [3]Guizhou Provincial Key Laboratory for Regenerative Medicine, Stem Cell and Tissue Engineering Research Center and Sino–US Joint Laboratory for Medical Sciences, Guizhou Medical University, Guiyang, Guizhou, People's Republic of China; [4]Research Center for Bioengineering and Sensing Technology, University of Science and Technology Beijing, Beijing, People's Republic of China; [5]Department of Internal Medicine, University of Utah and Salt Lake Veterans Affairs Medical Center, Salt Lake City, UT, USA; [6]Department of Colorectal Surgery, General Hospital of Ningxia Medical University, Yinchuan, Ningxia, People's Republic of China; [7]Cancer Center, Daping Hospital and Research Institute of Surgery, Third Military Medical University, Chongqing, People's Republic of China

Correspondence: Shu-Feng Zhou
Department of Pharmaceutical Sciences, College of Pharmacy, University of South Florida, 12901 Bruce B Downs Boulevard, Tampa, FL 33612, USA
Tel +1 813 974 6276
Fax +1 813 905 9885
Email szhou@health.usf.edu

Jia-Xuan Qiu
Department of Oral and Maxillofacial Surgery, The First Affiliated Hospital of Nanchang University, 17 Yongwaizheng St, Nanchang 330006, Jiangxi, People's Republic of China
Tel +86 791 8869 5069
Fax +86 791 8869 2745
Email qiujiaxuan@163.com

Abstract: Plumbagin (5-hydroxy-2-methyl-1,4-naphthoquinone; PLB), a naturally occurring naphthoquinone isolated from the roots of Plumbaginaceae plants, has been reported to possess anticancer activities in both in vitro and in vivo studies, but the effect of PLB on tongue squamous cell carcinoma (TSCC) is not fully understood. This study aimed to investigate the effects of PLB on cell cycle distribution, apoptosis, and autophagy, and the underlying mechanisms in the human TSCC cell line SCC25. The results have revealed that PLB exerted potent inducing effects on cell cycle arrest, apoptosis, and autophagy in SCC25 cells. PLB arrested SCC25 cells at the G_2/M phase in a concentration- and time-dependent manner with a decrease in the expression level of cell division cycle protein 2 homolog (Cdc2) and cyclin B1 and increase in the expression level of p21 Waf1/Cip1, p27 Kip1, and p53 in SCC25 cells. PLB markedly induced apoptosis and autophagy in SCC25 cells. PLB decreased the expression of the anti-apoptotic proteins B-cell lymphoma 2 (Bcl-2) and B-cell lymphoma-extra large (Bcl-xl) while increasing the expression level of the pro-apoptotic protein Bcl-2-associated X protein (Bax) in SCC25 cells. Furthermore, PLB inhibited phosphatidylinositol 3 kinase (PI3K)/protein kinase B (Akt)/mammalian target of rapamycin (mTOR), glycogen synthase kinase 3β (GSK3β), and p38 mitogen-activated protein kinase (p38 MAPK) pathways as indicated by the alteration in the ratio of phosphorylation level over total protein expression level, contributing to the autophagy inducing effect. In addition, we found that wortmannin (a PI3K inhibitor) and SB202190 (a selective inhibitor of p38 MAPK) strikingly enhanced PLB-induced autophagy in SCC25 cells, suggesting the involvement of PI3K- and p38 MAPK-mediated signaling pathways. Moreover, PLB induced intracellular reactive oxygen species (ROS) generation and this effect was attenuated by L-glutathione (GSH) and *N*-acetyl-L-cysteine (NAC). Taken together, these results indicate that PLB promotes cellular apoptosis and autophagy in TSCC cells involving p38 MAPK- and PI3K/Akt/mTOR-mediated pathways with contribution from the GSK3β and ROS-mediated pathways.

Keywords: TSCC, cell cycle, ROS, p38 MAPK, GSK3β

Introduction

Oral cavity and pharynx cancer is the eighth most common cancer worldwide, with 42,440 new cases in 2014, accounting for 4% of all cancer cases. Globally, an estimated 8,390 deaths from oral cavity and pharynx cancer are expected in 2014. The 5-year and 10-year relative survival rates are 62% and 51%, respectively. Among these cancers, tongue cancer is the most common one, with 13,590 new cases (32%) and 2,150 deaths (25%) in 2014.[1] Notably, tongue squamous cell carcinoma (TSCC) is the most prevalent histopathological type and exhibits aggressive behavior.[2]

Currently, radiation therapy and surgery, separately or in combination, are the standard treatments for early-stage TSCC, while chemotherapy is employed for advanced-stage TSCC.[1] Unfortunately, most TSCCs are diagnosed as advanced and metastatic diseases. Even after adapting all these treatments, many patients may still suffer from eating disorder, impaired language function, and even severe relapse.[3] Curing TSCC requires a comprehensive understanding of distinct biological events at the cellular and subcellular levels, which cover cell proliferation, cell survival, cell death, cell invasion, activation of oncogenes, loss of tumor suppressor genes, disrupted molecule interaction, and aberrant regulation of signaling pathways. The upcoming new insights will help identify new therapies and targets for TSCC treatment. As we all know, the malignance behavior of tumors is mostly due to the immortalized proliferation and altered programmed cell death of tumor cells. Biologically targeted therapy has become an optimistic maneuver to counteract TSCC, mainly by including adaptation of apoptosis and macroautophagy (hereafter referred to as 'autophagy'). The importance of apoptosis and autophagy in cancer treatment has been gradually accepted by most scholars.[4–7] During apoptosis, B-cell lymphoma 2 (Bcl-2) family-regulated intrinsic apoptosis is launched by the release of cytochrome c from the mitochondria into the cytosol, which can promote the formation of apoptosomes in the cytosol and subsequently activate the caspase cascade.[8–10] Failure in apoptosome formation is the major obstacle in the execution of apoptosis. Autophagy, the mammalian target of rapamycin (mTOR)-mediated cell death, involves a number of autophagy-related (Atg) proteins and other signaling pathways.[4–6] Autophagy has a paradoxical role in the occurrence and progression of tumors. While it is often recommended that a basal level of autophagy may render cell survival, continuous activation of autophagy may conversely lead to cell death by gradual self-degradation in cancer cells.[4–6] Notably, autophagy has not been investigated as often as apoptosis in TSCC and the role of autophagy in TSCC development and treatment is unclear, let alone the therapeutic and clinical implications.

Plumbagin (5-hydroxy-2-methyl-1,4-naphthoquinone; PLB) (Figure 1A), a naturally occurring yellow pigment, is isolated from *Plumbago zeylanica* L., *Juglans regia*, *Juglans cinerea*, and *Juglans nigra*.[11] PLB is notable for its high therapeutic efficiency and minimal side effects.[12] A quinone core is the functional group of PLB, which can render a variety of pharmacological activities including antifungal,[13] antibacterial,[14] antimalarial,[15] anti-inflammatory,[16] anti-atherosclerotic,[17] immunomodulatory,[18] and anticancer activities.[19] Based on the current in vitro and in vivo studies from our laboratory and other groups, PLB can lead to cell cycle arrest via its interaction with cell cycle checkpoints.[20] PLB can also induce cancer cell apoptosis and autophagy by inhibition of nuclear factor-κB (NF-κB) activation,[21] upregulation of p53 via c-Jun N-terminal kinase (JNK) phosphorylation,[22] and inhibition of phosphatidylinositol 3 kinase (PI3K)/protein kinase B (Akt)/mTOR pathway.[23,24] In addition, PLB can facilitate the generation of reactive oxygen species (ROS), which consequently leads to the killing of cancer cells.[25] Although PLB has shown potent anticancer effects in preclinical studies,[26] the underlying mechanism is not fully understood. In the present study, we examined the effects of PLB on cell cycle distribution, apoptosis, and autophagy and explored the underlying

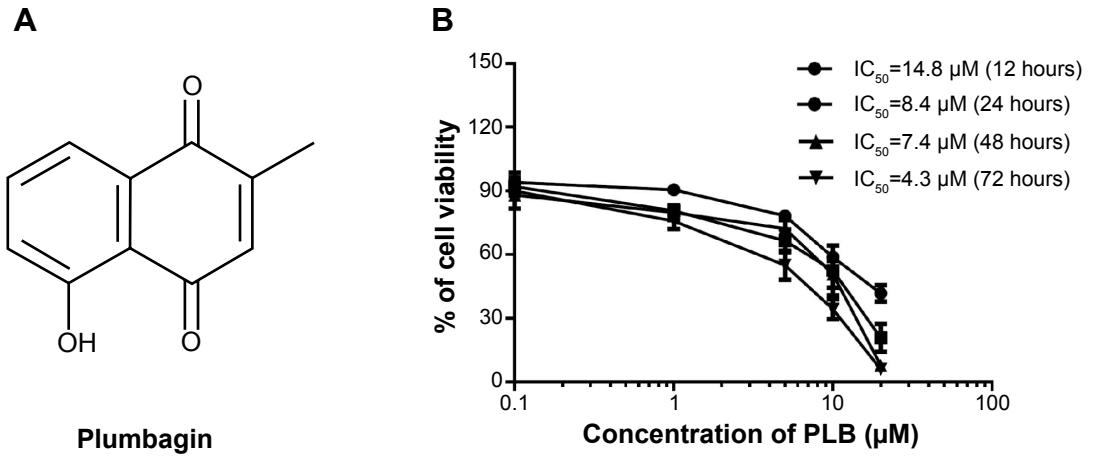

Figure 1 The chemical structure of PLB and the effect of PLB on the proliferation of SCC25 cells.
Notes: SCC25 cells were treated with PLB at concentrations ranging from 0.1 to 20 μM for 12, 24, 48, and 72 hours. (**A**) Chemical structure of PLB and (**B**) cell viability of SCC25 cells when treated with PLB at 0.1 to 20 μM for 12, 24, 48, and 72 hours. The cell viability was examined using the MTT assay.
Abbreviations: IC_{50}, half maximal inhibitory concentration; PLB, plumbagin; MTT, 3-(4,5-dimethylthiazol-2-yl)-2,5-diphenyltetrazolium bromide.

mechanism in human TSCC SCC25 cells with a focus on PI3K/Akt/mTOR signaling pathways.

Materials and methods

Chemicals and reagents

Dulbecco's Modified Eagle's Medium (DMEM) and Ham's F12 medium were obtained from Corning Cellgro Inc. (Herndon, VA, USA). PLB, L-glutathione (GSH, a ROS scavenger), *N*-acetyl-L-cysteine (NAC, a ROS scavenger), dimethyl sulfoxide (DMSO), liposaccharide, hydrocortisone, ammonium persulfate, D-glucose, propidium iodide (PI), ribonuclease (RNase A), protease inhibitor cocktail, radioimmunoprecipitation assay (RIPA) buffer, 3-(4,5-dimethylthiazol-2-yl)-2,5-diphenyltetrazolium bromide (MTT), bovine serum albumin, ethylenediaminetetraacetic acid (EDTA), 4-(2-hydroxyethyl)-1-piperazineethanesulfonic acid (HEPES), and Dulbecco's phosphate buffered saline (PBS) were purchased from Sigma-Aldrich Co. (St Louis, MO, USA). 4′,6-Diamidino-2-phenylindole (DAPI), 5-(and 6)-chloromethyl-2′,7′-dichlorodihydrofluorescein diacetate (CM-H_2DCFDA), wortmannin (WM; a potent, irreversible, and selective PI3K inhibitor and a blocker of autophagosome formation), SB202190 (4-(4-fluorophenyl)-2-(4-hydroxyphenyl)-5-(4-pyridyl)-1*H*-imidazole; a selective inhibitor of p38 mitogen-activated protein kinase [p38 MAPK] used as an autophagy inducer), and fetal bovine serum (FBS) were bought from Thermo Fisher Scientific Inc. (Waltham, MA, USA). The annexin V:phycoerythrin (PE) apoptosis detection kit was purchased from BD Biosciences Inc. (San Jose, CA, USA). Cyto-ID® Autophagy detection kit was obtained from Enzo Life Sciences Inc. (Farmingdale, NY, USA). Pierce™ bicinchoninic acid (BCA) protein assay kit, skim milk, and Western blotting substrate were bought from Thermo Fisher Scientific Inc. The polyvinylidene difluoride (PVDF) membrane was purchased from EMD Millipore Inc. (Billerica, MA, USA). Primary antibodies against human cell division cycle protein 2 homolog (Cdc2), cyclin B1, p53, p21/Waf1, p27 Kip1, Bcl-2-like protein 4/Bcl-2-associated X protein (Bax), Bcl-2, B-cell lymphoma-extra large (Bcl-xl), the p53 upregulated modulator of apoptosis (PUMA), cytochrome c, cleaved caspase 9, cleaved caspase 3, phospho-(p-)PI3K (Tyr458), PI3K, p-p38 (Thr180/Tyr182), p38, p-Akt (Ser473), Akt, p-mTOR (Ser2448), mTOR, beclin 1, microtubule-associated protein 1A/1B-light chain 3 (LC3-I), and LC3-II were all purchased from Cell Signaling Technology Inc. (Beverly, MA, USA). The antibody against human β-actin was obtained from Santa Cruz Biotechnology Inc. (Dallas, TX, USA).

Cell line and cell culture

The TSCC cell SCC25 was obtained from American Type Culture Collection (Manassas, VA, USA) and cultured in a 1:1 mixture of DMEM and Ham's F12 medium containing 1.2 g/L sodium bicarbonate, 2.5 mM L-glutamine, 15 mM HEPES,, and 0.5 mM sodium pyruvate and supplemented with 400 ng/mL hydrocortisone and 10% heat-inactivated FBS. The cells were maintained at 37°C in a 5% CO_2/95% air humidified incubator. PLB was dissolved in DMSO with a stock concentration of 100 mM, and was freshly diluted to the desired concentration with culture medium. The final concentration of DMSO was 0.05% (volume per volume [v/v]). The control cells received the vehicle only.

Cell viability assay

The MTT assay was performed to examine the effect of PLB on cell viability. Yellow MTT is reduced to purple formazan in the mitochondria of living cells. Briefly, SCC25 cells were seeded in 96-well culture plates at a density of 8,000 cells/well. After 24 hour incubation, the cells were treated with PLB at 0.1–20 μM for 12, 24, 48, and 72 hours. Following PLB treatment, 10 μL of MTT stock solution (5 mg/mL) was added to each well and incubated for a further 3 hours. The solution was then carefully aspirated and 100 μL DMSO was added into each well to dissolve the crystal. After shaking slowly for 30 minutes, the absorbance was measured using a Synergy™ H4 Hybrid microplate reader (BioTek Inc., Winooski, VT, USA) at the wavelengths of 560 nm and 670 nm (background). The half maximal inhibitory concentration (IC_{50}) values were determined using the relative viability over the PLB concentration curve.

Cell cycle distribution analysis

Flow cytometry was employed to determine the effect of PLB on the cell cycle of SCC25 cells. We used PI to stain the DNA and RNase A to hydrolyze the phosphodiester bond between the nucleotides. Briefly, SCC25 cells were seeded into six-well plates for attaching overnight. When the SCC25 cells reached ~80% confluence, the cells were then incubated with PLB at concentrations of 0.1, 1, and 5 μM for 24 hours. In separate experiments, SCC25 cells were treated with 5 μM PLB for 4, 8, 24, 48, and 72 hours. Cells were trypsinized and fixed with cold 70% ethanol at –20°C overnight. On the following day, the cells were incubated with 50 μg/mL PI and 25 μg/mL RNase A for 30 minutes in the dark at room temperature. A total of 1×10^4 events were subjected to cell cycle analysis using a flow cytometer (BD™ LSR II Analyzer; Becton Dickinson Immunocytometry Systems, San Jose, CA, USA).

Quantification of cellular apoptosis

We used the annexin V:PE apoptosis detection kit to measure the number of apoptotic cells after the cells were treated with PLB at different concentrations (0.1, 1, and 5 μM) for 24 hours. In separate experiments, SCC25 cells were treated with 5 μM PLB for 4, 8, 24, 48, and 72 hours. Annexin V is a 35 kDa Ca^{2+}-dependent phospholipid-binding protein that has a high affinity for negatively charged phospholipid phosphatidylserine, and binds to cells that are actively undergoing apoptosis with exposed phosphatidylserine. Cells that stain positive for annexin V:PE and negative for 7-aminoactinomycin D (7-AAD) are undergoing apoptosis; cells that stain positive for annexin V:PE and 7-AAD are either in the end stage of apoptosis, are undergoing necrosis, or are already dead; and cells that stain negative for both annexin V:PE and 7-AAD are alive and not undergoing measurable apoptosis. Briefly, cells were trypsinized and washed twice with cold PBS, and then resuspended in 1× binding buffer with 5 μL annexin V:PE and 5 μL of 7-AAD at a concentration of 1×10^5/mL cells in a total volume of 100 μL. The cells were gently mixed and incubated in the dark for 15 minutes at room temperature. Following that, a quota of 1× binding buffer (400 μL) was added to each test tube and the number of apoptotic cells was quantified by flow cytometry (BD™ LSR II Analyzer) within 1 hour.

Quantification of cellular autophagy

For autophagy detection, SCC25 cells were seeded in six-well plates and allowed to attach overnight. The cells were then treated with vehicle (0.05% DMSO, v/v) or PLB at concentrations of 0.1, 1, and 5 μM. In separate experiments, SCC25 cells were treated with 5 μM PLB for 4, 8, 24, 48, and 72 hours. Each live cell sample was trypsinized, washed by resuspending the cell pellet in 1× assay buffer (No ENZ-51031-K200; Enzo Life Sciences Inc.) and collected by centrifugation. Cells were resuspended in 250 μL of phenol red-free culture medium (No 1294895; Invitrogen, Carlsbad, CA, USA) containing 5% FBS, and 250 μL of the diluted Cyto-ID® Green stain solution (No ENZ-51031-K200; Enzo Life Sciences Inc.) was added to each sample and mixed well. Cells were incubated for 30 minutes at room temperature in the dark, collected by centrifugation, washed with 1× assay buffer, and resuspended in 500 μL fresh 1× assay buffer. Cells were analyzed using the green (FL1) channel of a flow cytometer (BD™ LSR II Analyzer).

Measurement of intracellular ROS levels

Intracellular levels of ROS were measured using a fluorometer using CM-H_2DCFDA according to the manufacturer's instructions. Upon oxidation by ROS, CM-H_2DCFDA is transformed to CM-DCF, which is highly fluorescent. Briefly, cells were seeded in 96-well plates at a density of 1×10^4 cells/well. After 24 hour treatment with PLB, the cells were incubated with CM-H_2DCFDA at 5 μM in PBS for 30 minutes. The fluorescence intensity was detected at wavelengths of 485 nm (excitation) and 530 nm (emission). In separate experiments, the intracellular ROS level was measured when SCC25 cells were treated with 5 μM PLB for 4, 8, 24, 48, and 72 hours. In addition, the effect of GSH and NAC on PLB-induced ROS generation was also examined. Cells were pre-treated with 1 mM GSH or 100 μM NAC for 1 hour, 5 μM PLB was added and incubated for a further 24 hours. LPS (100 ng/mL) was also included as a positive control. The fluorescence intensity was detected at wavelengths of 485 nm (excitation) and 530 nm (emission).

Western blotting analysis

The expression level of cellular proteins related to biological activities were determined using Western blotting assays. SCC25 cells were washed with PBS after 24 hour treatment with PLB, lysed with RIPA buffer (50 mmol HEPES at pH 7.5, 150 mmol NaCl, 10% glycerol, 1.5 mmol $MgCl_2$, 1% Triton-X 100, 1 mmol EDTA at pH 8.0, 10 mmol sodium pyrophosphate, and 10 mmol sodium fluoride) containing protease and phosphatase inhibitor cocktails. Protein concentrations were measured by Pierce™ BCA protein assay kit. Equal amounts of protein sample were electrophoresed on 7%–12% sodium dodecyl sulfate polyacrylamide gel electrophoresis (SDS-PAGE) mini-gel after thermal denaturation for 5 minutes at 95°C. Proteins were transferred onto immobilon PVDF membrane at 100 V for 2 hours at 4°C. Membranes were probed with indicated primary antibody overnight at 4°C and then blotted with the respective secondary antibody. Visualization was performed using the Bio-Rad ChemiDoc™ XRS system (Bio-Rad Laboratories Inc., Hercules, CA, USA) with electrochemiluminescence substrate and the blots were quantitatively analyzed by employing Image Lab 3.0. (Bio-Rad Laboratories Inc.). The protein level was normalized to the matching densitometric value of the internal control.

Confocal fluorescence microscopy

The cellular autophagy level was examined using the Cyto-ID® autophagy detection kit according to the manufacturer's instructions. Briefly, SCC25 cells were seeded in an eight-well chamber slide at 30% confluence. The cells were treated with PLB at 0.1, 1, and 5 μM for 24 hours. In separate experiments, SCC25 cells were treated with 5 μM PLB for 4, 8, 24, 48, and 72 hours. When the cells

reached ~60% confluence, they were washed by 1× assay buffer, following by incubation with 100 μL of microscopy dual detection reagent for 30 minutes at 37°C in the dark. After incubation, the cells were washed with 1× assay buffer to remove detection reagent and then the cells were examined using a Leica TCS SP2 laser scanning confocal microscopy (Leica Microsystems, Wetzlar, Germany) using a standard fluorescein isothiocyanate (FITC) filter set for imaging the autophagic signal at wavelengths of 405/488 nm.

Statistical analysis

Data are presented as the mean ± standard deviation (SD). Multiple comparisons were evaluated by one-way analysis of variance (ANOVA) followed by Tukey's multiple comparison procedure. Values of $P<0.05$ were considered statistically significantly different. All the assays were carried out in triplicate.

Results

PLB inhibits the proliferation of SCC25 cells

First, we detected the cytotoxicity of PLB in SCC25 cells using the MTT assay. The cells were incubated with PLB at various concentrations ranging from 0.1 to 20 μM for 12, 24, 48, and 72 hours. Compared with the control cells, the cellular viability of SCC25 cells were 94.0%, 90.5%, 78.3%, 58.8%, and 41.8% when exposed for 12 hours; 92.0%, 80.7%, 66.5%, 52.5%, and 20.8% when exposed for 24 hours; 88.0%, 79.8%, 72.3%, 50.8%, and 7.8% when exposed for 48 hours; and 85.5%, 75.8%, 55.0%, 34.3%, and 6.0% when exposed for 72 hours, to PLB at concentrations of 0.1, 1, 5, 10, and 20 μM, respectively. The IC_{50} values were 14.8, 8.4, 7.4, and 4.3 μM after 12, 24, 48, and 72 hours' incubation with PLB, respectively (Figure 1B). PLB inhibits SCC25 cells in a concentration- and time-dependent manner. Taken together, these results demonstrate that PLB has a potent antiproliferative effect on SCC25 cells.

PLB induces G_2/M arrest in SCC25 cells

In order to further explore the antiproliferative effect of PLB on SCC25 cells, the effect of PLB on the cellular cell cycle distribution was quantified using flow cytometric analysis. Firstly, the cells were treated with 0.1, 1, and 5 μM PLB for 24 hours (Figure 2A). Cell cycle distribution showed no significant change at 0.1 μM, whereas there was a significant increase in cell numbers in the G_2/M phase when treated with PLB at 5 μM (Figure 2B). At the same time, the cell population in the G_1 and S phases decreased correspondingly, which suggests that PLB at 5 μM is the most effective concentration related to the modulation of the cell cycle. Next, we conducted separate experiments to test the effect of PLB on cell cycle distribution over 72 hours (Figure 2C). There was no significant difference in the cell numbers in the G_1, S, and G_2/M phases after 4 and 8 hour treatment. However, there was a 0.8-, 1.9-, and 2.5-fold increase in G_2/M phase after cells were incubated with 5 μM PLB for 24, 48, and 72 hours, respectively ($P<0.001$; Figure 2D). Moreover, the cell numbers in both the G_1 and S phases were significantly decreased when treated with 5 μM PLB for 24, 48, and 72 hours, compared to the control cells. There was a 6.7%, 6.7%, and 8.4% reduction in the S phase and 3.0%, 3.9%, and 9.7% decrease in the G_1 phase when SCC25 cells were treated with 5 μM PLB for 24, 48, and 72 hours, respectively ($P<0.05$, $P<0.01$, or $P<0.001$; Figure 2D). Taken together, the results show that PLB possesses a potent inducing effect on cell cycle arrest, contributing to its anticancer effect.

PLB downregulates the expression of Cdc2 and cyclin B1 while upregulating the expression of p21 Waf1/Cip1, p27 Kip1, and p53 in SCC25 cells

As we had observed the regulatory effect of PLB on the cell cycle distribution in SCC25 cells, we next examined the effect of PLB on the expression of key cell cycle regulators, including Cdc2, cyclin B1, p21 Waf1/Cip1, p27 Kip1, and p53 in SCC25 cells by Western blotting assay. We observed variable alterations in the expression levels of cell cycle regulators (Figure 3A–D). The expression levels of Cdc2 and cyclin B1 were significantly decreased in a concentration-dependent manner. There were reductions of 26.0% and 39.5% in the expression levels of Cdc2 and cyclin B1 when treated with 1 μM PLB ($P<0.05$; Figure 3A and C), and decreases of 31.3% and 66.3% in the expression levels of Cdc2 and cyclin B1 when treated with 5 μM PLB, compared to the control cells ($P<0.01$; Figure 3A and C). In contrast, there was a concentration-dependent increase in the expression level of negative regulators of cell cycle progression. The expression level of p53 was increased by 2.0-, 2.1-, and 2.6-fold when cells were treated with 0.1, 1, and 5 μM PLB, respectively, compared to the control cells ($P<0.05$ or 0.01; Figure 3A and C). The expression level of p27 Kip1 was increased by 2.7-fold when treated with 5 μM PLB, compared to the control cells ($P<0.05$; Figure 3C). The expression level of p21 Waf1/Cip1 increased by 1.4-, 1.6-, and 1.8-fold when cells were incubated with 0.1, 1, and 5 μM PLB, respectively, compared to the control cells ($P<0.05$ or 0.01; Figure 3C).

We further examined the expression level of these proteins when SCC25 cells were incubated with 5 μM PLB for 6, 24, and 48 hours (Figure 3B and D). The expression level of Cdc2 was decreased by 31.5% and 34.0% at 24 and 48 hours, respectively ($P<0.05$; Figure 3B and D). The expression level of cyclin B1 was decreased by 17.0%, 23.0%, and 29.5% at 6, 24, and 48 hours, respectively, compared to the control cells ($P<0.05$ or 0.01; Figure 3B and D). The expression level of p53 was increased by 2.1-fold at 48 hours, compared to the control cells ($P<0.001$; Figure 3B and D). The expression level of p27 Kip1 was increased by 2.1- and 2.1-fold at 24 and 48 hours, respectively, compared to the control cells ($P<0.001$; Figure 3B and D). The expression level of p21 Waf1/Cip1 increased by 1.8- and 2.4-fold at 24 and 48 hours, respectively, compared to the control cells ($P<0.05$ or 0.01; Figure 3B and D). Taken together, the decreased expression level of Cdc2 and cyclin B1, key regulators for the G_2/M transition, provides an explanation for the PLB-induced G_2/M phase arrest. Moreover, the increased expression levels of p21 Waf1/Cip1, p27 Kip1, and p53 may contribute to the reduced cell population in the G_1 and S phases and G_2/M arrest.

PLB induces apoptosis of SCC25 cells via mitochondria-dependent pathway

To further probe into the anticancer effect of PLB on SCC25 cells, we quantitatively measured cellular apoptosis using flow cytometric analysis. The number of apoptotic cells at the basal level was 2%–3% in cells treated with the control vehicle only (0.05% DMSO, v/v; Figure 4A–D). When cells were treated with PLB at 0.1, 1, and 5 μM for 24 hours, the total percentage of apoptotic cells including in the early and late apoptosis stages were 5.3%, 5.7%, and 16.3%, respectively (Figure 4A). Notably, there was a 5.4-fold

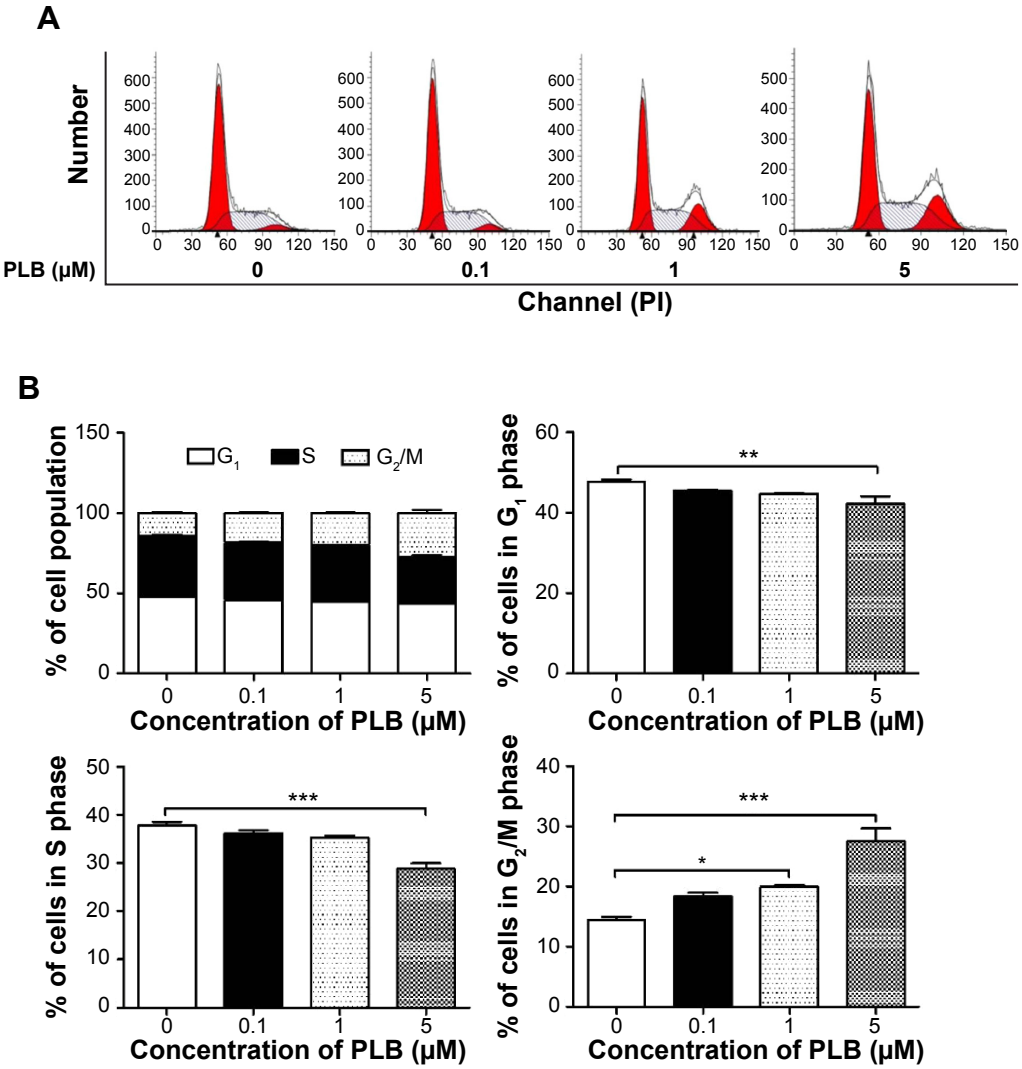

Figure 2 (*Continued*)

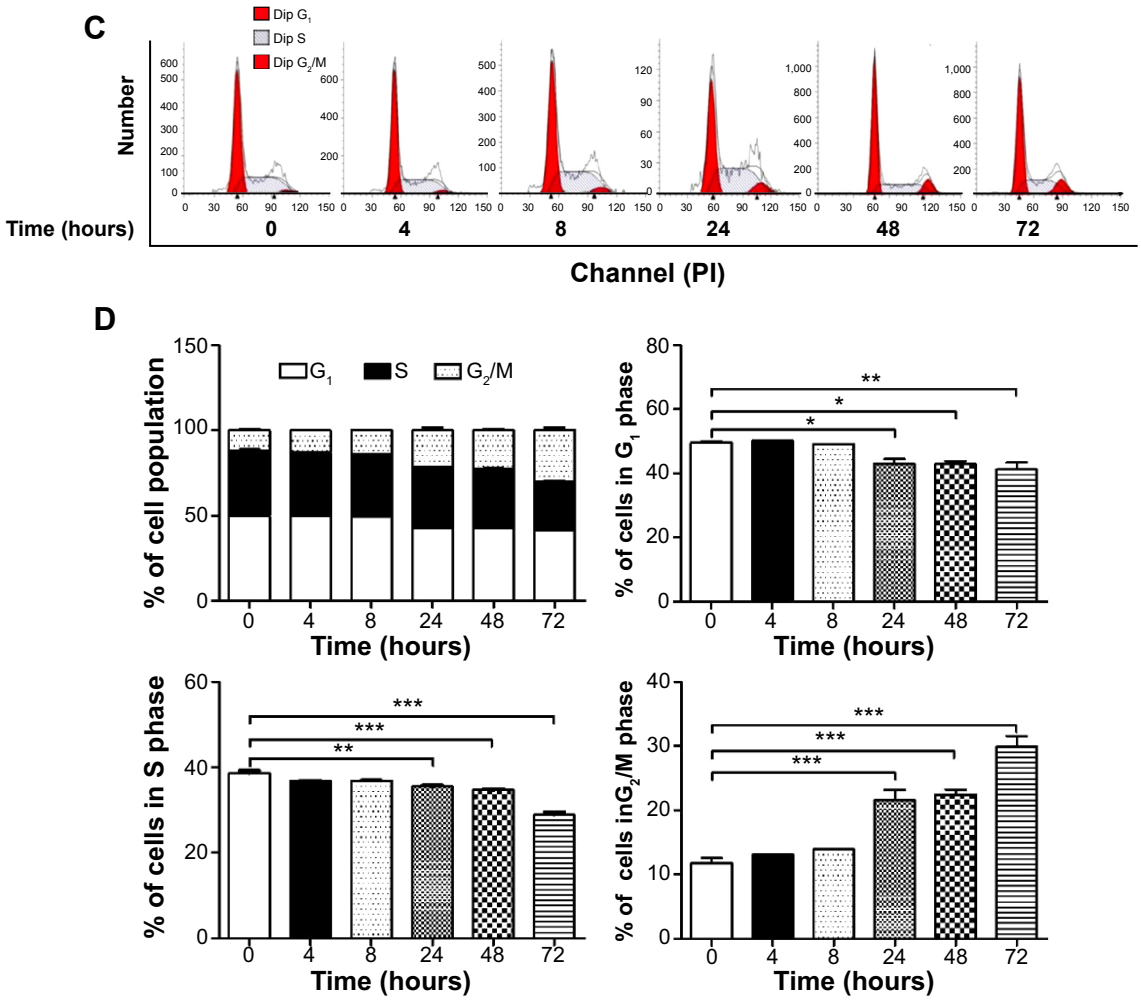

Figure 2 PLB induces G_2/M arrest in SCC25 cells.

Notes: (**A**) Flow cytometric histograms show the cell cycle distribution when the cells were treated with PLB at 0.1, 1, and 5 μM for 24 hours; (**B**) bar graphs show the cell cycle distribution when the cells were treated with PLB at 0.1, 1, and 5 μM for 24 hours; (**C**) flow cytometric histograms show the cell cycle distribution when the cells were treated with PLB at 5 μM over 72 hours; and (**D**) bar graphs show the cell cycle distribution when the cells were treated with PLB at 5 μM over 72 hours. Cells were stained with PI and subjected to flow cytometric analysis that collected 10,000 events. Data represent the mean ± SD of three independent experiments. *$P<0.05$; **$P<0.01$; and ***$P<0.001$ by one-way ANOVA.

Abbreviations: ANOVA, analysis of variance; Dip, diploid; PI, propidium iodide; PLB, plumbagin; SD, standard deviation.

increase in apoptotic cells when treated with 5 μM PLB, compared to the control cells ($P<0.001$; Figure 4B). In addition, the effect of PLB on the apoptosis of SCC25 cells was examined when cells were treated for 4, 8, 24, 48, and 72 hours (Figure 4C). Cells incubated with 5 μM PLB increased the percentage of apoptotic cells in a time-dependent manner. The percentage of apoptotic cells was increased from 3.5% at the basal level (time 0) to 5.0%, 22.8%, 37.7%, 62.9%, and 68.0% with the treatment of 5 μM PLB for 4, 8, 24, 48, and 72 hours, respectively ($P<0.001$; Figure 4D). These results indicate that PLB induces apoptotic cell death of SCC25 cells in a concentration- and time-dependent manner.

Since we have observed the pro-apoptotic effect of PLB in SCC25 cells, we further examined the expression level of relevant proteins responsible for this phenomenon. Using Western blotting, we checked the expression levels of the pro-apoptotic protein Bax and the anti-apoptotic proteins Bcl-2 and Bcl-xl. The successful execution of mitochondria-mediated apoptosis (also known as 'intrinsic apoptosis') requires a variety of proteins and molecules. When stimuli from the outer membrane activate one or more members of BH3-only protein family, cellular apoptosis is initiated. Bcl-2-antagonist/killer-1 (Bak) and Bax oligomers gather gradually, which then leads to the release of cytochrome c to the cytosol. Eventually, apoptosomes are formed and this activates caspase 9 and caspase 3 in a positive feedback manner. SCC25 cells were treated with PLB at 0.1, 1, and 5 μM for 24 hours (Figure 5A). The expression level of Bax was increased by 4.6-, 5.3-, and 7.6-fold when cells were treated with 0.1, 1, and 5 μM PLB for 24 hours, respectively ($P<0.01$ or 0.001; Figure 5C). In contrast, the expression level of Bcl-2 was decreased by 12.0% and 28.7% when

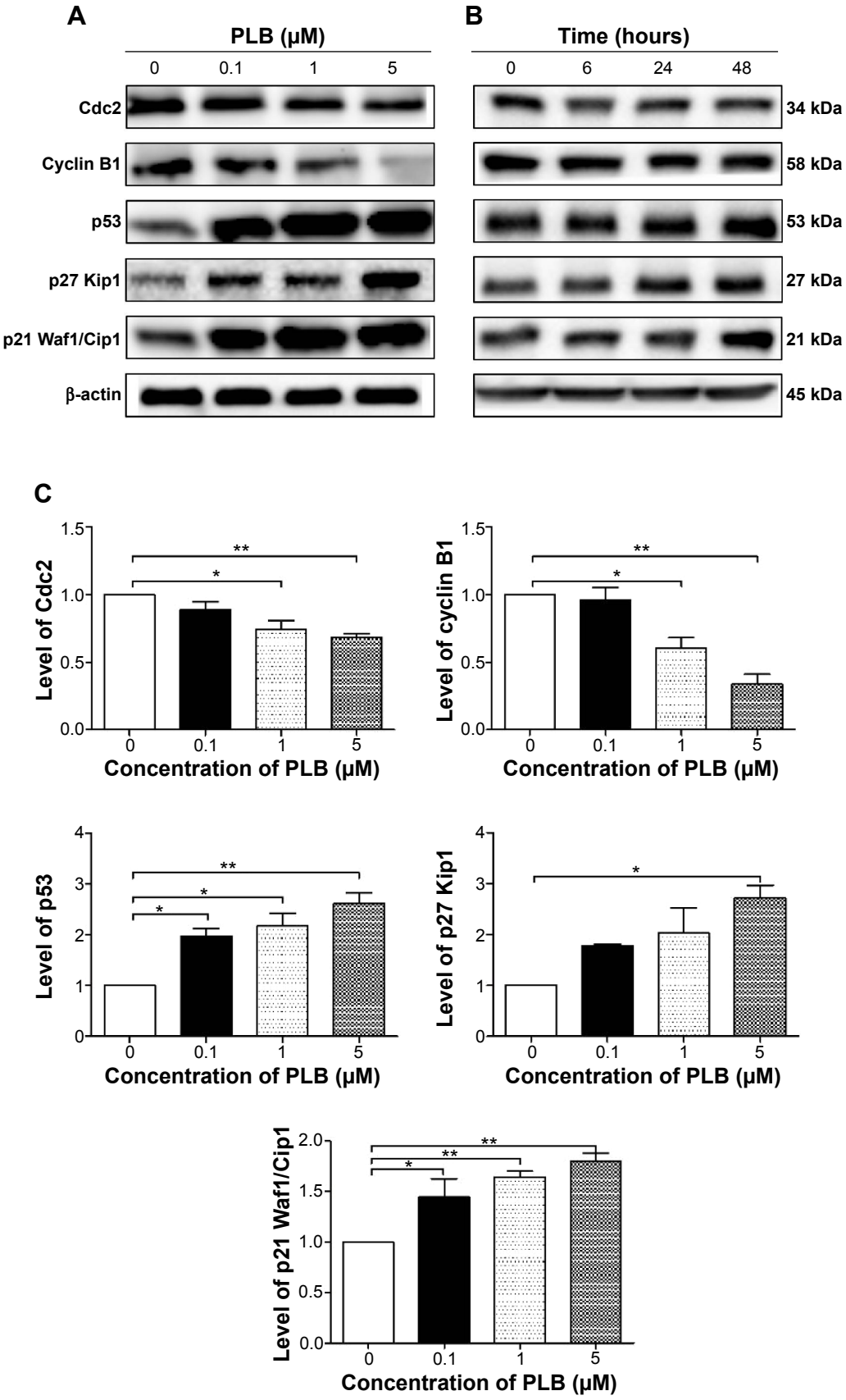

Figure 3 (*Continued*)

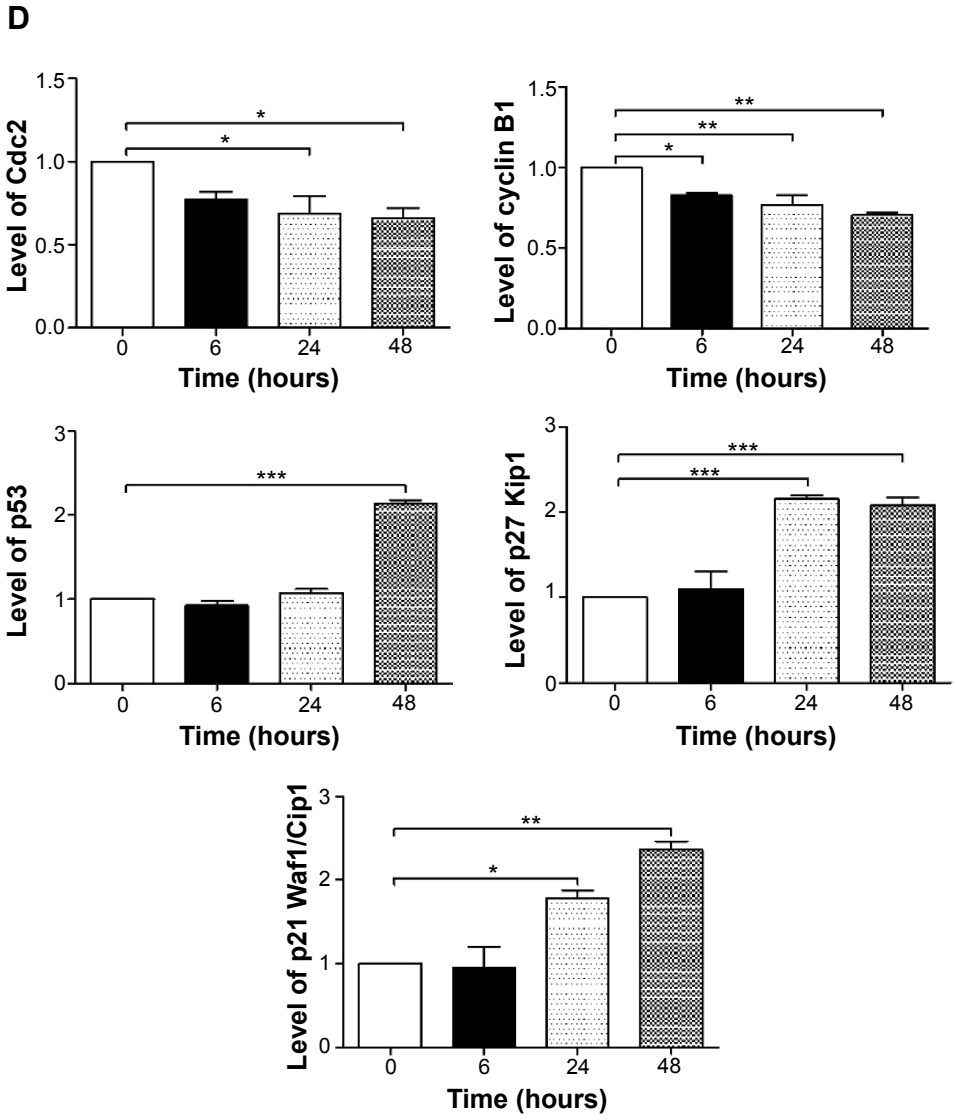

Figure 3 Effect of PLB on the expression levels of cell cycle-related proteins in SCC25 cells.
Notes: The expression levels of Cdc2, cyclin B1, p53, p27 kip1, and p21 Waf1/Cip1 were determined by Western blotting. β-actin was used as the internal control. (**A**) Representative blots show the expression levels of Cdc2, cyclin B1, p53, p27 Kip1, and p21 Waf1/Cip1 when the cells were treated with PLB at 0.1, 1, and 5 μM for 24 hours; (**B**) representative blots show the expression levels of Cdc2, cyclin B1, p53, p27 Kip1, and p21 Waf1/Cip1 when the cells were treated with PLB at 5 μM for 6, 24, and 48 hours; (**C**) bar graphs show the expression levels of Cdc2, cyclin B1, p53, p27 Kip1, and p21 Waf1/Cip1 when the cells were treated with PLB at 0.1, 1, and 5 μM for 24 hours; and (**D**) bar graphs show the expression levels of Cdc2, cyclin B1, p53, p27 Kip1, and p21 Waf1/Cip1 when the cells were treated with PLB at 5 μM for 6, 24, and 48 hours. β-actin was used as the internal control. Data represent the mean ± SD of three independent experiments. *$P<0.05$; **$P<0.01$; and ***$P<0.001$ by one-way ANOVA.
Abbreviations: ANOVA, analysis of variance; PLB, plumbagin; SD, standard deviation; Cdc2, cell division cycle protein 2 homolog.

cells were incubated with PLB at 1 and 5 μM for 24 hours, respectively ($P<0.05$ or 0.001; Figure 5C). The Bax/Bcl-2 ratio was significantly increased by 4.8-, 5.8-, and 10.4-fold when cells were treated with 0.1, 1, and 5 μM PLB for 24 hours, respectively, compared to control cells ($P<0.05$ or 0.001; Figure 5C). In addition, the expression level of Bcl-xl was reduced by 33.0% when cells were treated with PLB at 5 μM for 24 hours, compared to control cells ($P<0.05$; Figure 5C).

Moreover, the effect of PLB on the expression of PUMA was also examined due to its crucial role in the regulation of anti-apoptotic proteins. Incubation the cells with 5 μM PLB increased the expression level of PUMA by 1.6-fold ($P<0.01$; Figure 5C). Further, the expression level of cytochrome c was increased by 1.2-, 1.8-, and 1.7-fold with the treatment of PLB at 0.1, 1, and 5 μM, respectively ($P<0.05$ or 0.001; Figure 5C). The expression levels of cleaved caspase 9 and cleaved caspase 3 were both increased by various amounts (Figure 5C). In separate experiments, we observed that PLB regulates the expression of apoptotic proteins in a time-dependent manner (Figure 5B). Briefly, SCC25 cells were incubated with 5 μM PLB for 6, 24, and 48 hours.

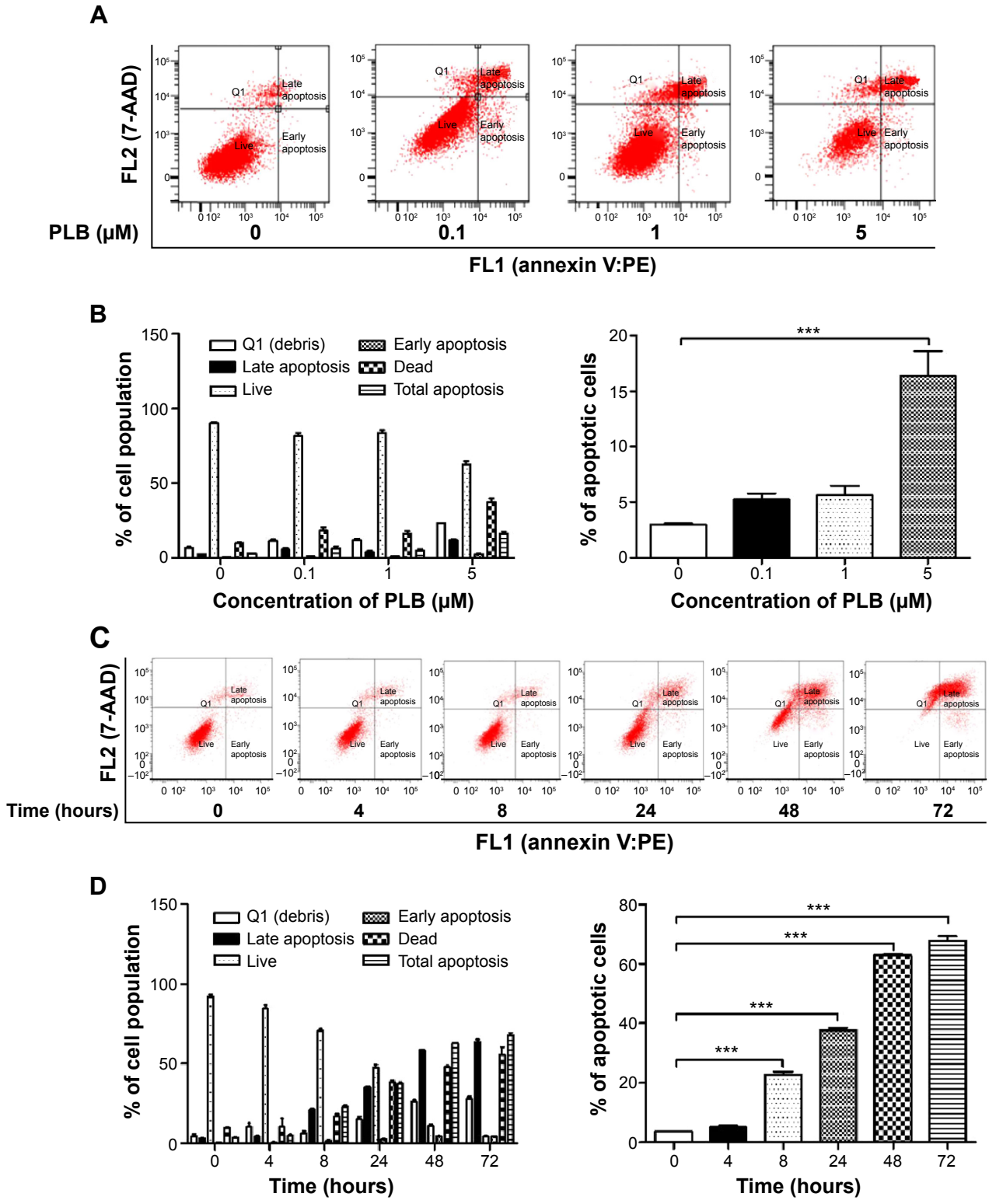

Figure 4 PLB induces apoptosis in SCC25 cells.

Notes: (**A**) Flow cytometric plots show cells in the live, early apoptosis, and late apoptosis stages when the cells were treated with PLB at 0.1, 1, and 5 μM for 24 hours; (**B**) bar graphs show the percentage of specific cell populations (live, early apoptosis, and late apoptosis) when the cells were treated with PLB at 0.1, 1, and 5 μM for 24 hours; (**C**) flow cytometric plots show live, early apoptosis, and late apoptosis when the cells were treated with PLB at 5 μM for 4, 8, 24, 48, and 72 hours; and (**D**) bar graphs show the percentage of specific cell populations (live, early apoptosis, and late apoptosis) when the cells were treated with PLB at 5 μM for 4, 8, 24, 48, and 72 hours. Cells were double stained with annexin V:PE and 7-AAD and subjected to flow cytometric analysis that collected 10,000 events. Data are the mean ± SD of three independent experiments. ***$P<0.001$ by one-way ANOVA.

Abbreviations: 7-AAD, 7-aminoactinomycin D; ANOVA, analysis of variance; PLB, plumbagin; SD, standard deviation; FL, fluorescence channel; PE, phycoerythrin; Q1, debris.

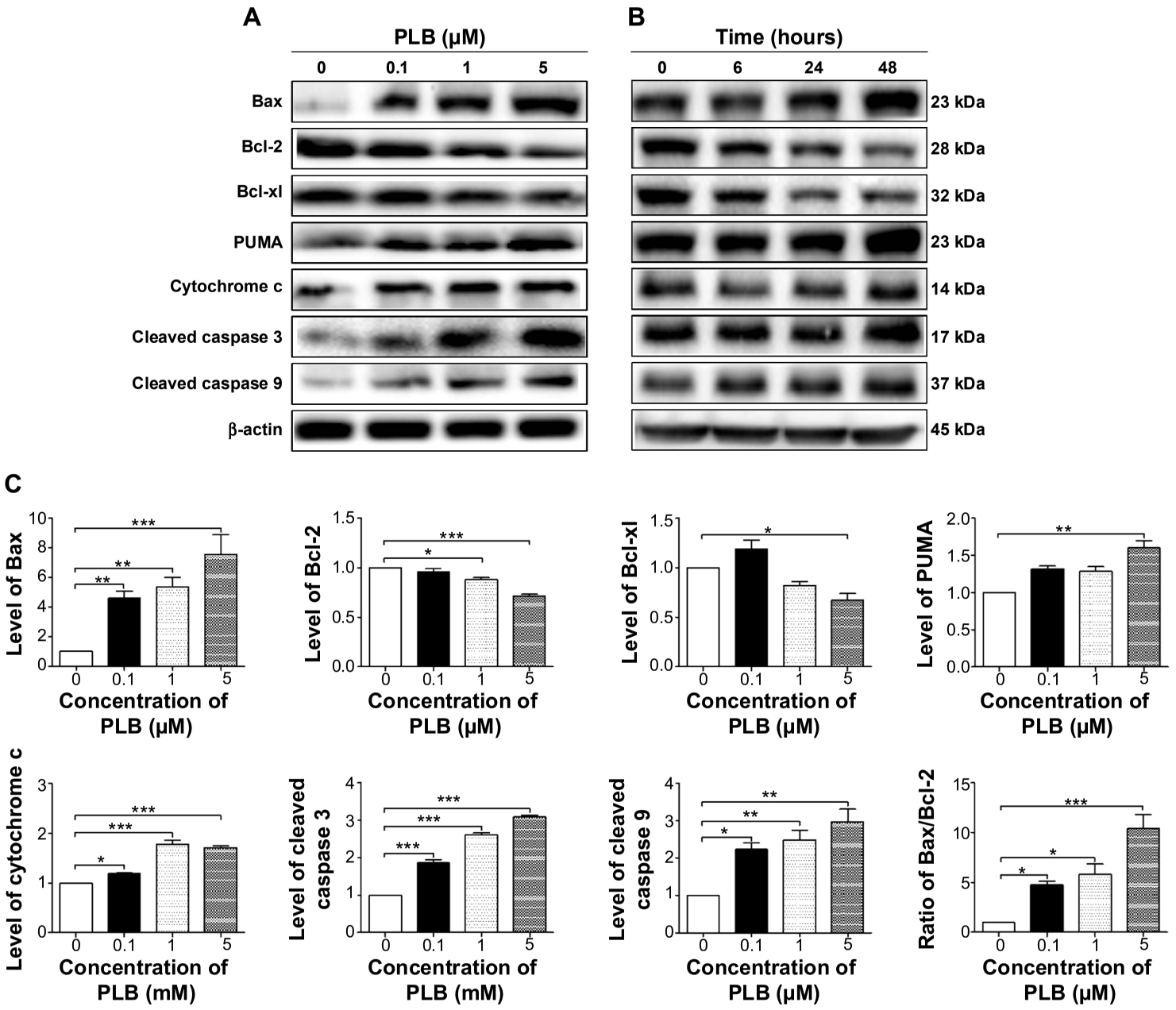

Figure 5 (*Continued*)

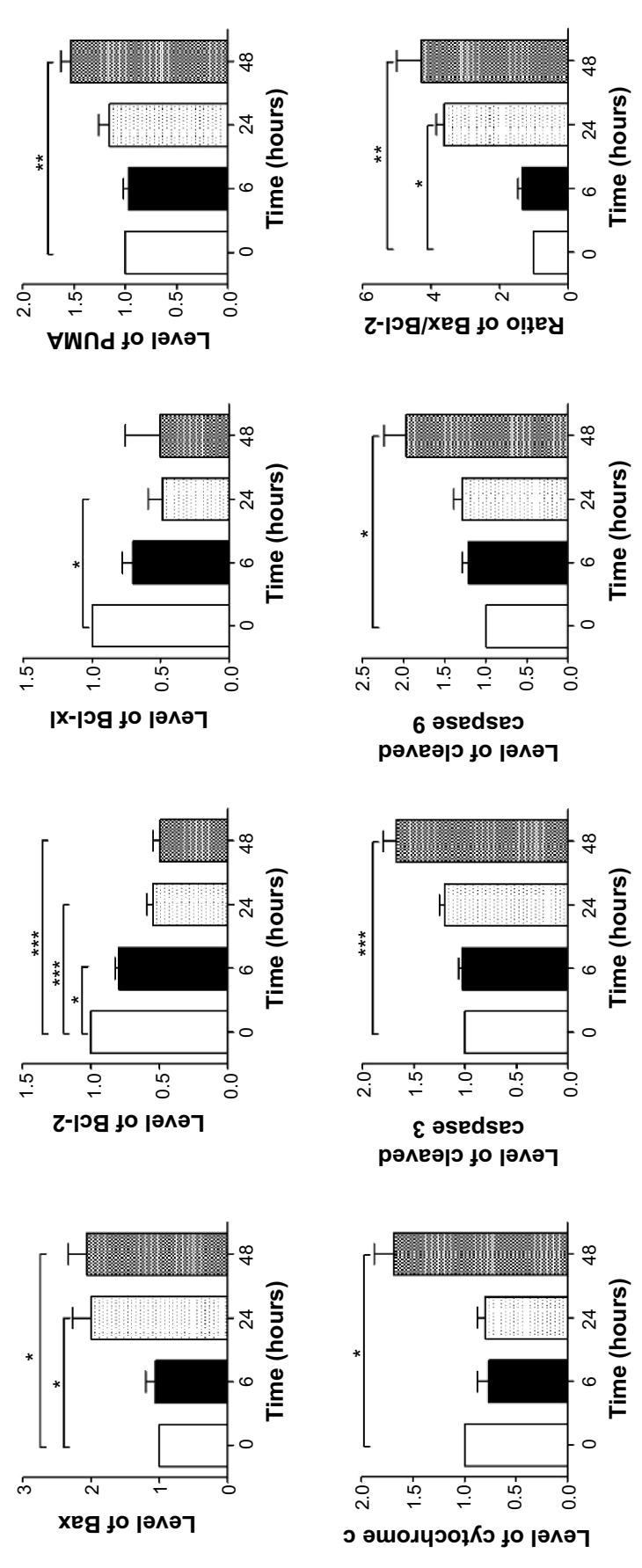

Figure 5 Effect of PLB on the expression levels of apoptosis-related proteins in SCC25 cells.

Notes: The expression levels of Bax, Bcl-2, Bcl-xl, PUMA, cytochrome c, cleaved caspase 3, and cleaved caspase 9 in SCC25 cells determined by Western blotting assay. β-actin was used as the internal control. (**A**) Representative blots show the expression levels of Bax, Bcl-2, Bcl-xl, PUMA, cytochrome c, cleaved caspase 3, and cleaved caspase 9 when the cells were treated with PLB at 0.1, 1, and 5 μM for 24 hours; (**B**) representative blots show the expression levels of Bax, Bcl-2, Bcl-xl, PUMA, cytochrome c, cleaved caspase 3, and cleaved caspase 9 when the cells were treated with PLB at 5 μM for 6, 24, and 48 hours; (**C**) bar graphs show the expression levels of Bax, Bcl-2, Bcl-xl, PUMA, cytochrome c, cleaved caspase 3, and cleaved caspase 9 in SCC25 cells treated with PLB at 0.1, 1, and 5 μM for 24 hours; and (**D**) bar graphs show the expression levels of Bax, Bcl-2, Bcl-xl, PUMA, cytochrome c, cleaved caspase 3, and cleaved caspase 9 when the cells were treated with PLB at 5 μM for 6, 24, and 48 hours. β-actin was used as the internal control. Data are the mean ± SD of three independent experiments. *$p<0.05$; **$p<0.01$; and ***$p<0.001$ by one-way ANOVA.

Abbreviations: ANOVA, analysis of variance; PLB, plumbagin; SD, standard deviation; Bax, Bcl-2-associated X protein; Bcl-2, B-cell lymphoma 2; Bcl-xl, B-cell lymphoma-extra large; PUMA, p53 upregulated modulator of apoptosis.

The expression level of Bax was increased by 2.0- and 2.1-fold when SCC25 were treated with 5 μM PLB for 24 and 48 hours, respectively, compared to control cells ($P<0.05$; Figure 5D). The expression level of Bcl-2 was decreased by 20.3%, 45.0%, and 50.3% when treated for 6, 24, and 48 hours, respectively ($P<0.05$ or 0.001; Figure 5D). The Bax/Bcl-2 ratio was increased by 3.6- and 4.3-fold when cells were treated with 5 μM PLB for 24 and 48 hours, respectively ($P<0.05$ or 0.01; Figure 5D). Taken together, these results demonstrate an upregulating role of PLB in the expression of pro-apoptotic proteins in SCC25 cells.

PLB induces autophagy in SCC25 cells

Autophagy and apoptosis are the major modes of programmed cell death; they interact with each other. Autophagy usually acts ahead of apoptosis when cells encounter outer membrane stresses. Since we have observed PLB-induced apoptosis in SCC25 cells, we next examined the effect of PLB on the autophagy of SCC25 cells using flow cytometric analysis and confocal microscopy. SCC25 cells were exposed to 0.1, 1, and 5 μM PLB for 24 hours (Figure 6A). The percentage of autophagic cells at the basal level was 3.7% for SCC25 cells. The autophagy level was increased by 2.1- and 4.1-fold when cells were exposed to 1 and 5 μM PLB, respectively, compared to control cells ($P<0.01$ or 0.001; Figure 6C). Furthermore, we examined the effect of PLB on the autophagy of SCC25 cells over 72 hours. Briefly, SCC25 cells were incubated with 5 μM PLB for 4, 8, 24, 48, and 72 hours (Figure 6B). The autophagy level was increased by 1.9-, 4.9-, 5.2-, and 5.5-fold when cells were treated for 8, 24, 48, and 72 hours, respectively, compared to control cells ($P<0.001$; Figure 6D). Next, we applied 10 μM WM and 20 μM SB202190 to examine the effect of PLB on the cellular autophagy level (Figure 7A). The results showed that the autophagy level was increased by 1.8- and 2.7-fold in cells treated with SB202190 + PLB or WM + PLB, respectively, compared with PLB alone (Figure 7B). These results suggest that PLB-induced autophagy may be, at least in part, ascribed to the regulation of the PI3K- and p38 MAPK-mediated signaling pathways.

In addition, we determined the autophagy-inducing effects of PLB in SCC25 cells using confocal microscopic examination. In comparison to the control cells, PLB treatment induced a significant concentration-dependent increase in autophagic cells (Figure 8A). There was a 1.2- and 1.4-fold increase in the autophagic death of SCC25 cells when treated with PLB at 1 and 5 μM for 24 hours, respectively ($P<0.01$ or 0.001; Figure 8B). Treatment of cells with PLB at 0.1 μM did not significantly affect the autophagy of SCC25 cells. Furthermore, the autophagy-inducing effect of PLB on SCC25 cells over 72 hours was also examined (Figure 8C). There was a time-dependent increase in autophagy when SCC25 cells were treated with 5 μM PLB. Compared to the control cells, 5 μM PLB led to a 1.1-, 1.3-, 1.5-, and 1.8-fold increase in the autophagic death of SCC25 cells after 8, 24, 48, and 72 hour incubation, respectively ($P<0.001$; Figure 8D). These results show that PLB induces autophagy in SCC25 in a concentration- and time-dependent manner with an involvement of the PI3K- and p38 MAPK-mediated signaling pathways.

PLB negatively regulates p38 MAPK and PI3K/Akt/mTOR axis

Upon the observation that WM and SB202190 can enhance PLB-induced autophagy, we further investigated the underlying mechanisms for the autophagy-inducing effect of PLB on SCC25 cells. First, we examined the phosphorylation levels of PI3K at Tyr458, and p38 MAPK at Thr180/Tyr182, which are well-documented as upstream signaling molecules of the Akt/mTOR pathway and play important roles in the regulation of cell proliferation and death. PI3K catalyzes the formation of phosphatidylinositol-3,4,5-triphosphate via phosphorylation of phosphatidylinositol, phosphatidylinositol-4-phosphate, and phosphatidylinositol-4,5-bisphosphate. Various stimuli, such as growth factors and hormones, can initiate this phosphorylation event, which in turn modulates cell proliferation, cell cycle, cell migration, and cell survival. In our study, PLB markedly inhibited the phosphorylation of PI3K at Tyr458 in a concentration-dependent manner, compared to the control cells (Figures 9A and 10). The phosphorylation level of PI3K at Tyr458 was decreased by 25.0%, 37.5%, and 42.5% when the cells were exposed to 0.1, 1, and 5 μM PLB, respectively, compared to the control cells ($P<0.01$ or 0.001; Figure 10). The ratio of p-PI3K/PI3K was decreased by 54.0%, 34.5%, and 62.1% when the cells were treated with 0.1, 1, and 5 μM PLB, respectively, compared to the control cells ($P<0.05$ or 0.01; Figure 10).

Glycogen synthase kinase 3β (GSK3β), an enzyme involved in the control of glycogen metabolism, has been revealed to take a part in tumor proliferation, growth, survival, metastasis, apoptosis, and autophagy.[27–31] Incubation of SCC25 cells with PLB for 24 hours suppressed GSK3β activation, with increased levels of p-GSK3β at Ser9 in a concentration-dependent manner (Figure 9A). In comparison to the control cells, there was a 1.5- and 1.6-fold increase in the phosphorylation level of GSK3β at Ser9 when treated with 1 and 5 μM PLB for 24 hours, respectively. The p-GSK3β/GSK3β ratio was increased by 1.3- and 2.0-fold, respectively ($P<0.001$; Figure 10). However, the expression

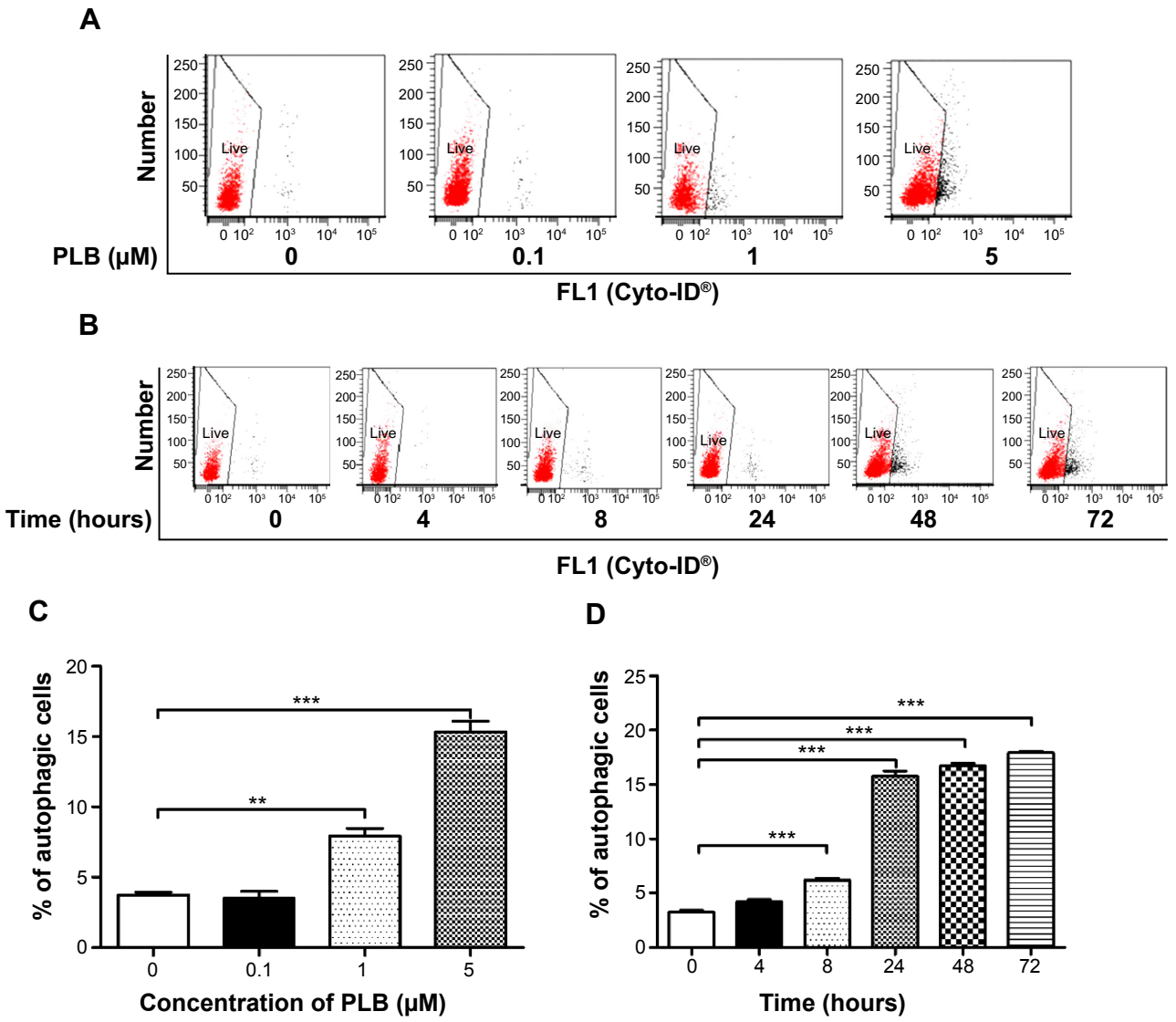

Figure 6 PLB induces autophagic cell death in SCC25 cells determined by flow cytometry.

Notes: Cells were treated with PLB at concentrations of 0.1, 1, and 5 μM for 24 hours or treated with 5 μM PLB for 4, 8, 24, 48, and 72 hours. Then cell samples were subjected to flow cytometric analysis. (**A**) flow cytometric dot plots show autophagy when the cells were treated with PLB at 0.1, 1, and 5 μM for 24 hours; (**B**) flow cytometric dot plots show autophagy when cells were treated with PLB at 5 μM for 4, 8, 24, 48, and 72 hours; (**C**) bar graphs show the percentage of autophagic cells when the cells were treated with PLB at 0.1, 1, and 5 μM for 24 hours; and (**D**) bar graphs show the percentage of autophagic cells when the cells were treated with PLB at 5 μM for 4, 8, 24, 48, and 72 hours. Cells were stained with Cyto-ID® to detect autophagy using a flow cytometer that collected 10,000 events. Data are presented as the mean ± SD of three independent experiments. $^{**}P<0.01$; and $^{***}P<0.001$ by one-way ANOVA.

Abbreviations: ANOVA, analysis of variance; PLB, plumbagin; SD, standard deviation; FL, fluorescence channel.

level of total GSK3β had no significant change. Furthermore, p38 MAPK is closely related to inflammatory response and genotoxic stresses.[32] p38 MAPK is a member of the MAPK family, which includes Erk1/2 and JNK. p38 MAPK consists of six subunits: α1, α2, β1, β2, γ, and δ. These subunits have 60% homologous sequence with different phenotypes and substrates.[33] p38 MAPK is involved in multiple biological processes, including apoptosis,[34] inflammation,[35] ischemia reperfusion injury,[36] phenotype differentiation,[37] and tumor development.[38] MAP kinase kinase 3 (MKK3), MKK6, and MKK4 can activate p38 MAPK by phosphorylation at Thr180 and Tyr182. Consequently, activated p38 MAPK can phosphorylate MAP kinase-activated protein kinase 2 and several transcription factors that trigger the expression of a number of target genes.[39] p38 MAPK plays a paradoxical role as a regulator of apoptosis, and it can either mediate cell survival or cell death depending not only on the type of stimulus but also in a cell type-specific context.[34,40] In our study, we observed an inhibitory effect of PLB on the activation of p38 MAPK at Thr180/Tyr182 in SCC25 cells (Figure 9A). When SCC25 cells were exposed to 5 μM PLB, it showed a significant 46.5% decrease in cell numbers. The ratio of p-p38 MAPK/p38 MAPK was decreased by 60.4% when treated with 5 μM PLB, compared to the

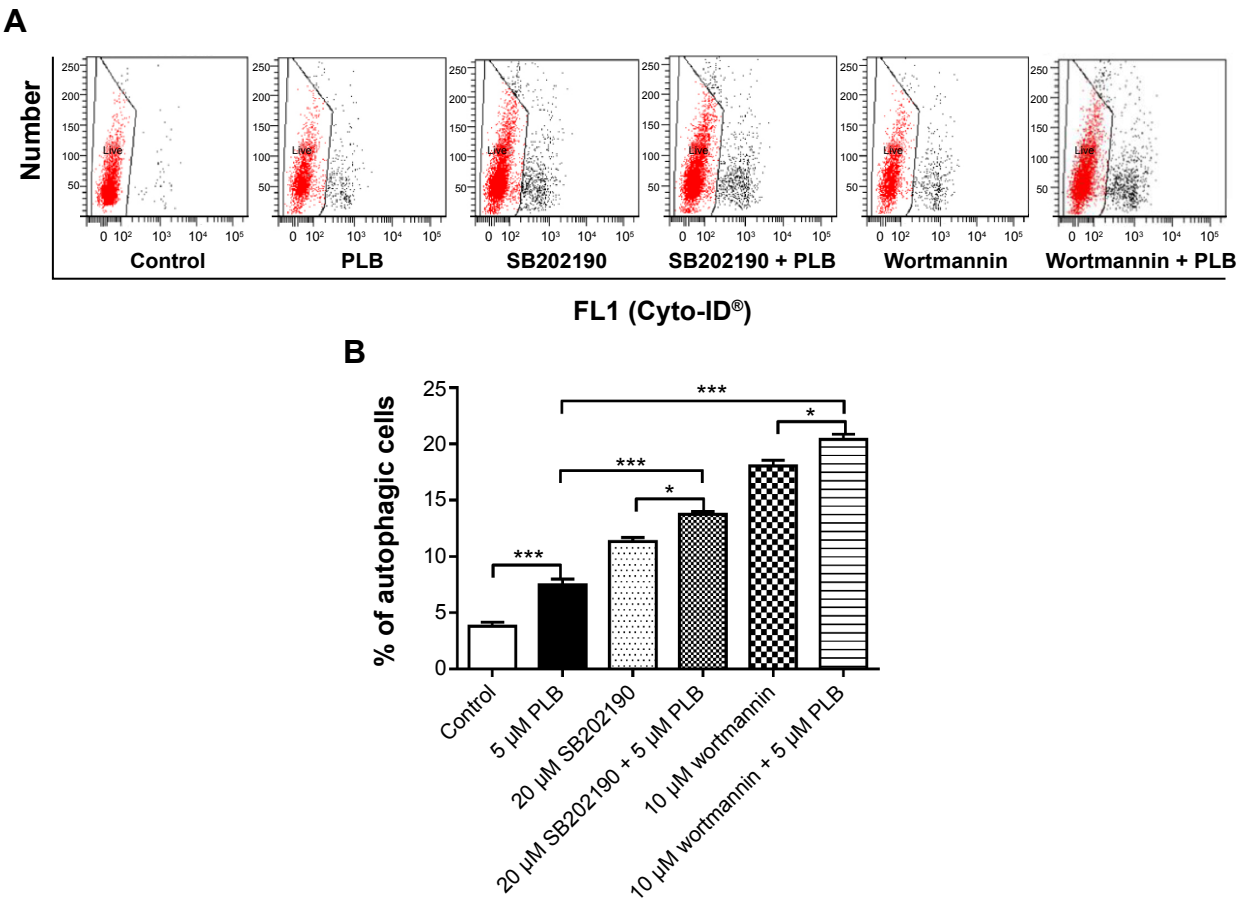

Figure 7 Effect of wortmannin (PI3K inhibitor) and SB202190 (p38 MAPK inhibitor) on PLB-induced autophagy in SCC25 cells.
Notes: Cells were treated with PLB at 5 μM for 24 hours with or without 10 μM wortmannin or 20 μM SB202190. The autophagy inducing effect of PLB was determined by flow cytometry using Cyto-ID® as the stain for autophagic vacuoles. (**A**) Flow cytometric dot plots show autophagy in SCC25 cells treated with PLB, wortmannin, SB202190, wortmannin + PLB, or SB202190 + PLB for 24 hours and (**B**) bar graphs show the percentage of autophagic cells in SCC25 cells treated with PLB, wortmannin, SB202190, wortmannin + PLB, or SB202190 + PLB for 24 hours. Cells were stained with green fluorescent Cyto-ID® to detect autophagy using a flow cytometer that collected 10,000 events. Data are the mean ± SD of three independent experiments. *$P<0.05$; and ***$P<0.001$ by one-way ANOVA.
Abbreviations: ANOVA, analysis of variance; MAPK, mitogen-activated protein kinase; PI3K, phosphatidylinositide 3 kinase; PLB, plumbagin; SD, standard deviation; FL, fluorescence channel.

control cells ($P<0.01$ or 0.001; Figure 10). These findings demonstrate that PLB inhibits the phosphorylation of PI3K at Tyr199 and p38 MAPK at Thr180/Tyr182 but enhances the phosphorylation of GSK3β at Ser9 in SCC25 cells, contributing to the increase in autophagy flux.

We further examined the regulatory effect of PLB on the phosphorylation of Akt at Ser473 and mTOR at Ser2448 in SCC25 cells (Figure 9A). Akt takes a part in the regulation of various signaling downstream pathways, including cell proliferation, growth, survival, angiogenesis, and chemoresistance.[41] As a downstream effector of PI3K, Akt can activate mTOR, while mTORC2 phosphorylates Akt at Ser473 and stimulates Akt phosphorylation at Thr308 by 3-phosphoinositide-dependent protein kinase 1, leading to full Akt activation.[41] mTOR plays a key role in cell growth, autophagic cell death, and homeostasis.[42] mTOR is phosphorylated at Ser2448 via the PI3K/Akt signaling pathway and autophosphorylated at Ser2481.[42] mTOR inhibition promotes dissociation of mTOR from the complex of Atg13 with Unc-51 like autophagy activating kinase 1 (ULK1) and ULK2. This releases ULK1/2 to activate the focal adhesion kinase family interacting protein of 200 kDa (FIP200), a protein critical for autophagosome formation and autophagy initiation.[42] In comparison to the control cells, the phosphorylation level of Akt at Ser473 was decreased by 71.3% after treatment with PLB at 5 μM for 24 hours ($P<0.001$; Figure 10). However, there was a slight increase in the expression of Akt after treatment with 1 μM PLB for 24 hours ($P<0.05$; Figure 10). Moreover, the ratio of p-Akt/Akt was significantly decreased in SCC25 cells treated with PLB. The ratio was decreased from 0.7 at base level to 0.4 and 0.3 when cells were treated with PLB at 1 and 5 μM for 24 hours, respectively. Further, the phosphorylation level of mTOR was decreased by 28.3%, 30.3%, and 74.3% when exposed to PLB at 0.1, 1, and 5 μM for 24 hours, respectively ($P<0.01$ or 0.001; Figure 10). The

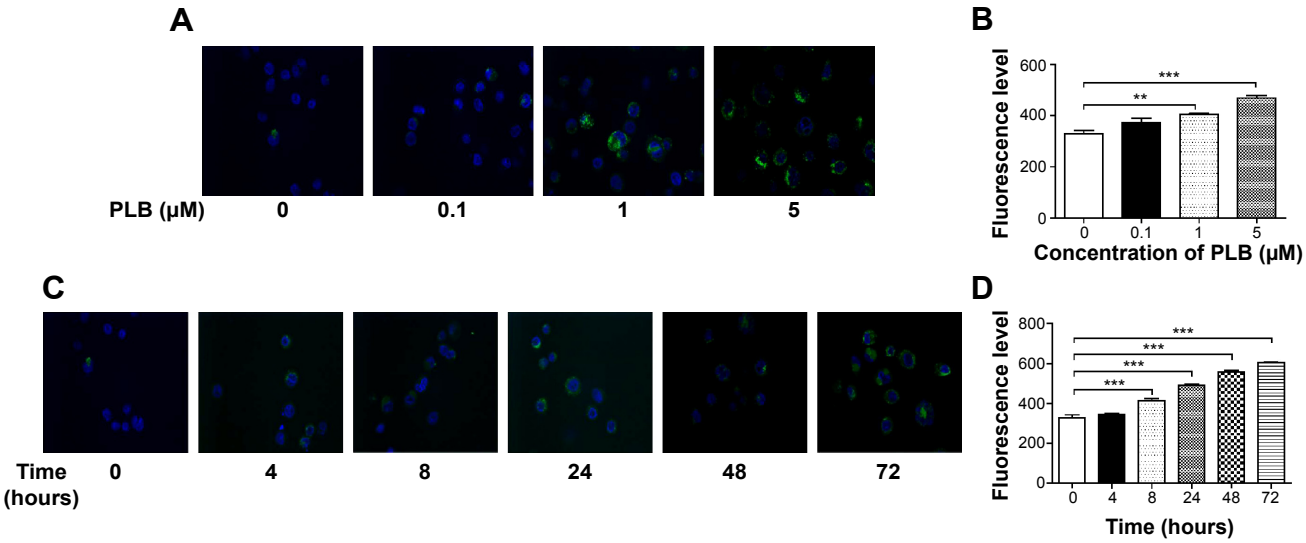

Figure 8 PLB induces autophagic cell death in SCC25 cells determined by confocal microscopy.
Notes: Cells were treated with PLB at concentrations of 0.1, 1, and 5 μM for 24 hours or treated with 5 μM PLB for 4, 8, 24, 48, and 72 hours. Then, cell samples were subjected to confocal microscopic examination. (**A**) Confocal microscopic images show autophagy in SCC25 cells treated with PLB at 0.1, 1, and 5 μM for 24 hours; (**B**) bar graphs show the percentage of autophagic SCC25 cells treated with PLB at 0.1, 1, and 5 μM for 24 hours; (**C**) confocal microscopic images show autophagy in SCC25 cells treated with 5 μM PLB over 72 hours; and (**D**) bar graphs show the percentage of autophagic SCC25 cells over 72 hours. Cells were stained with green fluorescent Cyto-ID® to detect autophagy using a flow cytometer that collected 10,000 events. Data represent the mean ± SD. $^{**}P<0.01$; and $^{***}P<0.001$ by one-way ANOVA.
Abbreviations: ANOVA, analysis of variance; PLB, plumbagin; SD, standard deviation.

expression of total mTOR was increased by 2.8- and 2.7-fold when treated with 1 and 5 μM PLB, respectively. The ratio of p-mTOR/mTOR was remarkably decreased from 2.85 at the basal level to 0.7, 1.7, and 0.2 when cells were treated with PLB at 0.1, 1, and 5 μM for 24 hours, respectively ($P<0.05$ or 0.001; Figure 10).

Finally, we examined the effect of PLB on the expression level of beclin 1 and LC3-I/II. Autophagy is tightly regulated by beclin 1 (a mammalian homolog of yeast Atg6), which forms a complex with vacuolar protein sorting 34 (Vps34, also called class III PI3K), and serves as a platform for recruitment of other Atgs that are critical for autophagosome formation.[43,44] Upon autophagy initiation, LC3 is cleaved at the C-terminus by Atg4 to form the cytosolic LC3-I.[45] LC3-I is consequently proteolytically cleaved and lipidated by Atg3 and Atg7 to form LC3-II, which localizes to the autophagosome membrane. The expression level of beclin 1 was increased by 1.7-fold when the cells were treated with 5 μM PLB for 24 hours ($P<0.001$; Figure 10). After 24 hour treatment with PLB, our Western blotting analysis revealed two clear bands of LC3-I and II. There was a concentration-dependent increase in the expression of LC3-II. Compared to the control cells, there was a 2.2- and 2.7-fold increase in the level of LC3-II when the cells were treated with PLB at 1 and 5 μM for 24 hours, respectively ($P<0.01$; Figure 10). Interestingly, treatment of SCC25 cells with PLB also increased the expression of LC3-I at 5 μM. In addition, the ratio of LC3-II/I was remarkably increased by 2.4-fold after treatment with PLB at 5 μM for 24 hours ($P<0.001$; Figure 10). These findings indicate that PLB exhibits a potent autophagy-inducing effect on SCC25 cells with contribution, at least in part, from the inhibition of p38 MAPK and the PI3K/Akt/mTOR signaling pathways.

In separate experiments, we examined the phosphorylation levels of GSK3β, PI3K, p38 MAPK, Akt, and mTOR when SCC25 cells were treated with 5 μM PLB for 6, 24, and 48 hours (Figures 9B and 11). The phosphorylation level of PI3K was decreased by 45.0% when treated with 5 μM PLB for 48 hours ($P<0.05$; Figure 11), whereas the expression level of total PI3K was increased by 2.1-fold when compared to the control cells ($P<0.01$; Figure 11). The ratio of p-PI3K/PI3K was decreased by 61% when treated with 5 μM PLB for 48 hours ($P<0.05$; Figure 11). The level of p-GSK3β was increased by 1.7-fold when the cells were treated with 5 μM PLB for 48 hours ($P<0.001$; Figure 11). Although the expression level of GSK3β did not show statistically significant change, the ratio of p-GSK3β/GSK3β was increased by 2.0-fold after treatment with 5 μM PLB for 48 hours ($P<0.001$; Figure 11). The phosphorylation level of p38 MAPK was decreased by 59% when treated with 5 μM PLB for 48 hours ($P<0.001$; Figure 11), whereas the expression level of total p38 MAPK was not statistically significantly different. The ratio of p-p38 MAPK/p38 MAPK was significantly decreased by 58.4% when SCC25 cells were treated with 5 μM PLB for 48 hours

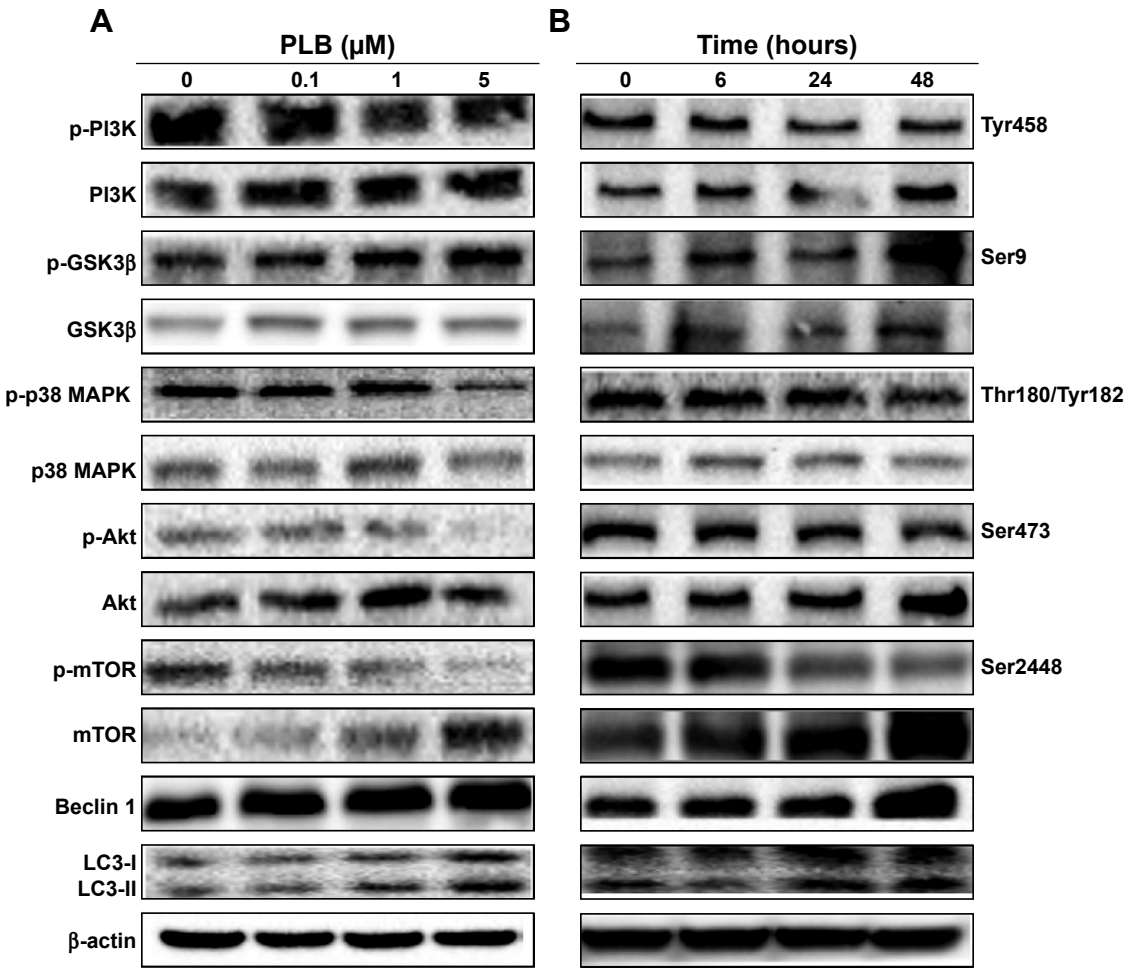

Figure 9 Effect of PLB on the expression level of autophagy-associated proteins in SCC25 cells.

Notes: The phosphorylation levels of PI3K, GSK3β, p38 MAPK, and Akt, and the total levels of mTOR, beclin 1, LC3-I, and LC3-II in SCC25 cells determined by Western blotting assay. β-actin was used as the internal control. (**A**) Representative blots show the expression levels of p-PI3K, PI3K, p-GSK3β, GSK3β, p-p38 MAPK, p38 MAPK, p-Akt, Akt, p-mTOR, mTOR, beclin 1, LC3-I, and LC3-II in SCC25 cells treated with PLB at 0.1, 1, and 5 μM for 24 hours and (**B**) representative blots show the expression levels of p-PI3K, PI3K, p-GSK3β, GSK3β, p-p38 MAPK, p38 MAPK, p-Akt, Akt, p-mTOR, mTOR, beclin 1, LC3-I, and LC3-II in SCC25 cells treated with PLB at 5 μM for 6, 24, and 48 hours. β-actin was used as the internal control.

Abbreviation: Akt, protein kinase B; GSK3β, glycogen synthase kinase 3β; LC3, microtubule-associated protein 1 light chain 3; MAPK, mitogen-activated protein kinase; mTOR, mammalian target of rapamycin; PI3K, phosphatidylinositide 3 kinase; PLB, plumbagin.

($P<0.01$; Figure 11). Moreover, the level of p-Akt was decreased by 49.3% and 47.0% when the cells were treated with 5 μM PLB for 24 and 48 hours, respectively ($P<0.05$; Figure 11). The expression level of total Akt was increased by 2.9- and 2.5-fold when SCC25 cells were treated with 5 μM PLB for 24 and 48 hours, respectively ($P<0.01$). The ratio of p-Akt/Akt was significantly decreased by 29.0%, 71.3%, and 71.7% when the cells were treated with 5 μM PLB for 6, 24, and 48 hours, respectively ($P<0.05$ or 0.001; Figure 11). Notably, the phosphorylation level of mTOR was significantly decreased by 43.3%, 47.7%, and 51.0% when SCC25 cells were treated with 5 μM PLB for 6, 24, and 48 hours, respectively, compared to the control cells ($P<0.01$ or 0.001; Figure 11). The expression level of total mTOR was increased by 1.6-fold when SCC25 cells were treated with 5 μM PLB for 48 hours ($P<0.001$; Figure 11). The ratio of p-mTOR/mTOR was decreased by 26.7%, 40%, and 69.7% when SCC25 cells were treated with 5 μM PLB for 6, 24, and 48 hours, respectively, compared to the control cells ($P<0.05$, 0.01, or 0.001; Figure 11). Furthermore, the expression level of LC3-II was increased by 1.7- and 2.1-fold when SCC25 cells were treated with 5 μM PLB for 24 and 48 hours, respectively, compared to the control cells ($P<0.01$ or 0.001; Figure 11). The ratio of LC3-II/I was significantly increased by 2.7-fold when SCC25 cells were incubated with 5 μM PLB for 48 hours ($P<0.01$; Figure 11). In addition, the expression level of beclin1 was increased by 1.8-fold after SCC25 cells were treated with 5 μM PLB for 48 hours ($P<0.01$; Figure 11). Collectively, these results show that PLB regulates the PI3K/Akt/mTOR axis in a concentration- and time-dependent manner toward autophagy with the involvement of GSK3β and p38 MAPK.

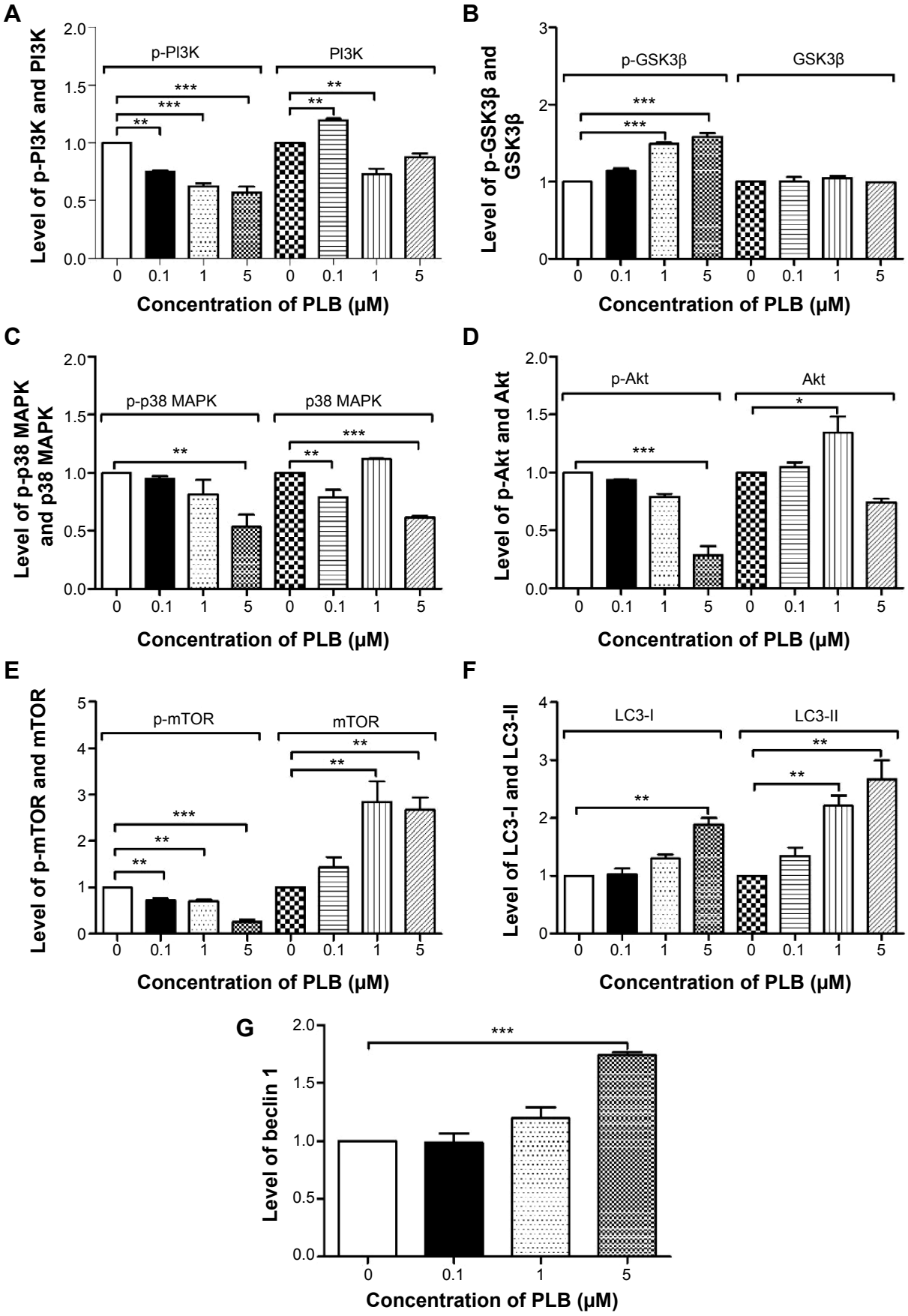

Figure 10 (*Continued*)

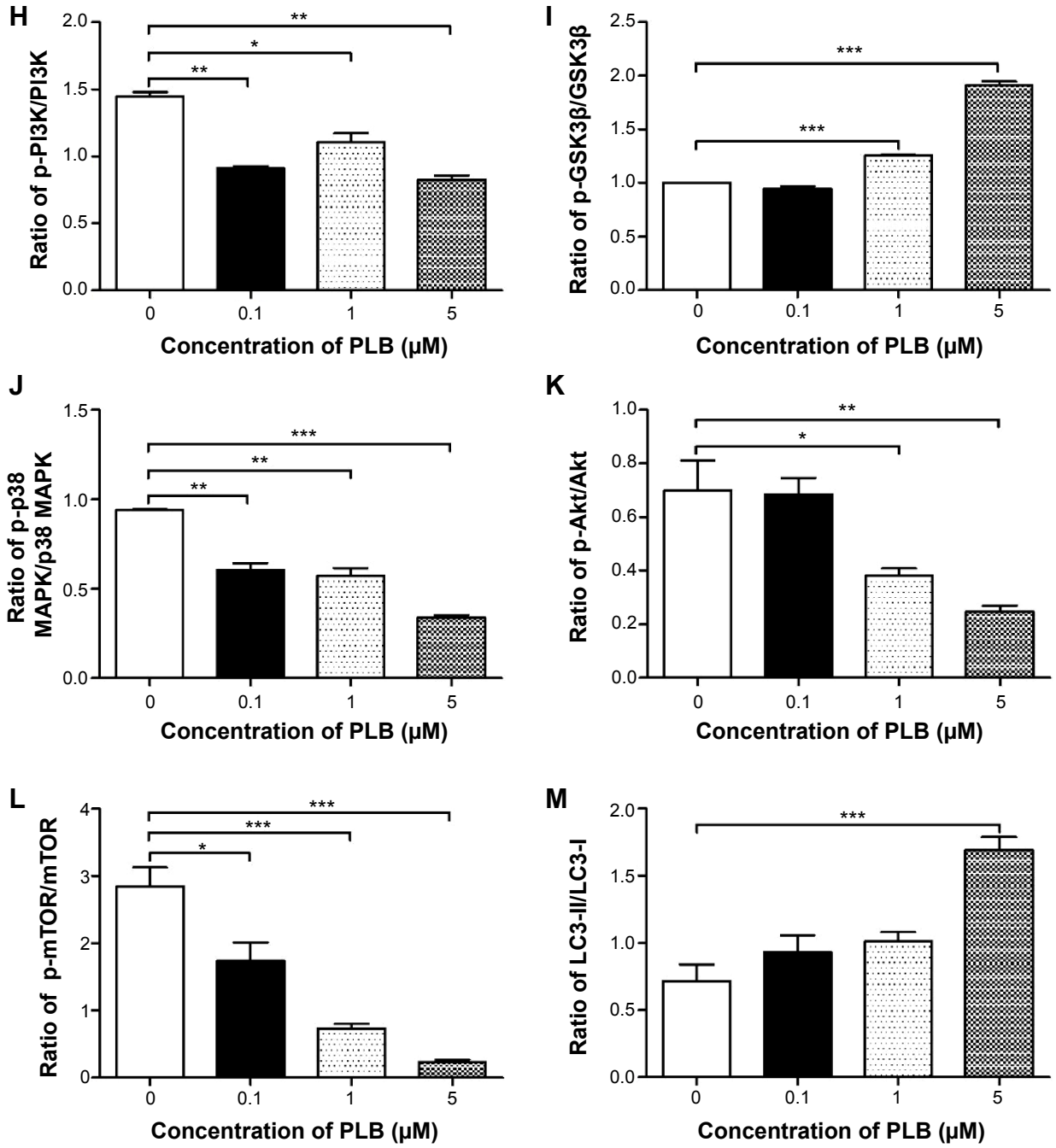

Figure 10 Effect of PLB concentration on the expression levels of autophagy-associated proteins in SCC25 cells.

Notes: : (**A**) Bar graph shows the expression levels of p-PI3K and PI3K in SCC25 cells treated with PLB at 0.1, 1, and 5 μM; (**B**) bar graph shows the expression levels of p-GSK3β and GSK3β in SCC25 cells treated with PLB at 0.1, 1, and 5 μM; (**C**) bar graph shows the expression levels of p-p38 MAPK and p38 MAPK in SCC25 cells treated with PLB at 0.1, 1, and 5 μM; (**D**) bar graph shows the expression levels of p-Akt and Akt in SCC25 cells treated with PLB at 0.1, 1, and 5 μM; (**E**) bar graph shows the expression levels of p-mTOR and mTOR in SCC25 cells treated with PLB at 0.1, 1, and 5 μM; (**F**) bar graph shows the expression levels of LC3-I and LC3-II in SCC25 cells treated with PLB at 0.1, 1, and 5 μM; (**G**) bar graph shows the expression levels of beclin 1 in SCC25 cells treated with PLB at 0.1, 1, and 5 μM; (**H**) bar graph shows the ratio of p-PI3K over PI3K in SCC25 cells treated with PLB at 0.1, 1, and 5 μM; (**I**) bar graph shows the ratio of p-GSK3β over GSK3β in SCC25 cells treated with PLB at 0.1, 1, and 5 μM; (**J**) bar graph shows the ratio of p-p38 MAPK over p38 MAPK in SCC25 cells treated with PLB at 0.1, 1, and 5 μM; (**K**) bar graph shows the ratio of p-Akt over Akt in SCC25 cells treated with PLB at 0.1, 1, and 5 μM; (**L**) bar graph shows the ratio of p-mTOR over mTOR in SCC25 cells treated with PLB at 0.1, 1, and 5 μM; and (**M**) bar graph shows the ratio of LC3-II over LC3-I in SCC25 cells treated with PLB at 0.1, 1, and 5 μM. β-actin was used as the internal control. Data are the mean ± SD of three independent experiments. *$P<0.05$; **$P<0.01$; and ***$P<0.001$ by one-way ANOVA.

Abbreviations: ANOVA, analysis of variance; PLB, plumbagin; SD, standard deviation; Akt, protein kinase B; GSK3β, glycogen synthase kinase 3β; LC3, microtubule-associated protein 1 light chain 3; MAPK, mitogen-activated protein kinase; mTOR, mammalian target of rapamycin; PI3K, phosphatidylinositide 3 kinase.

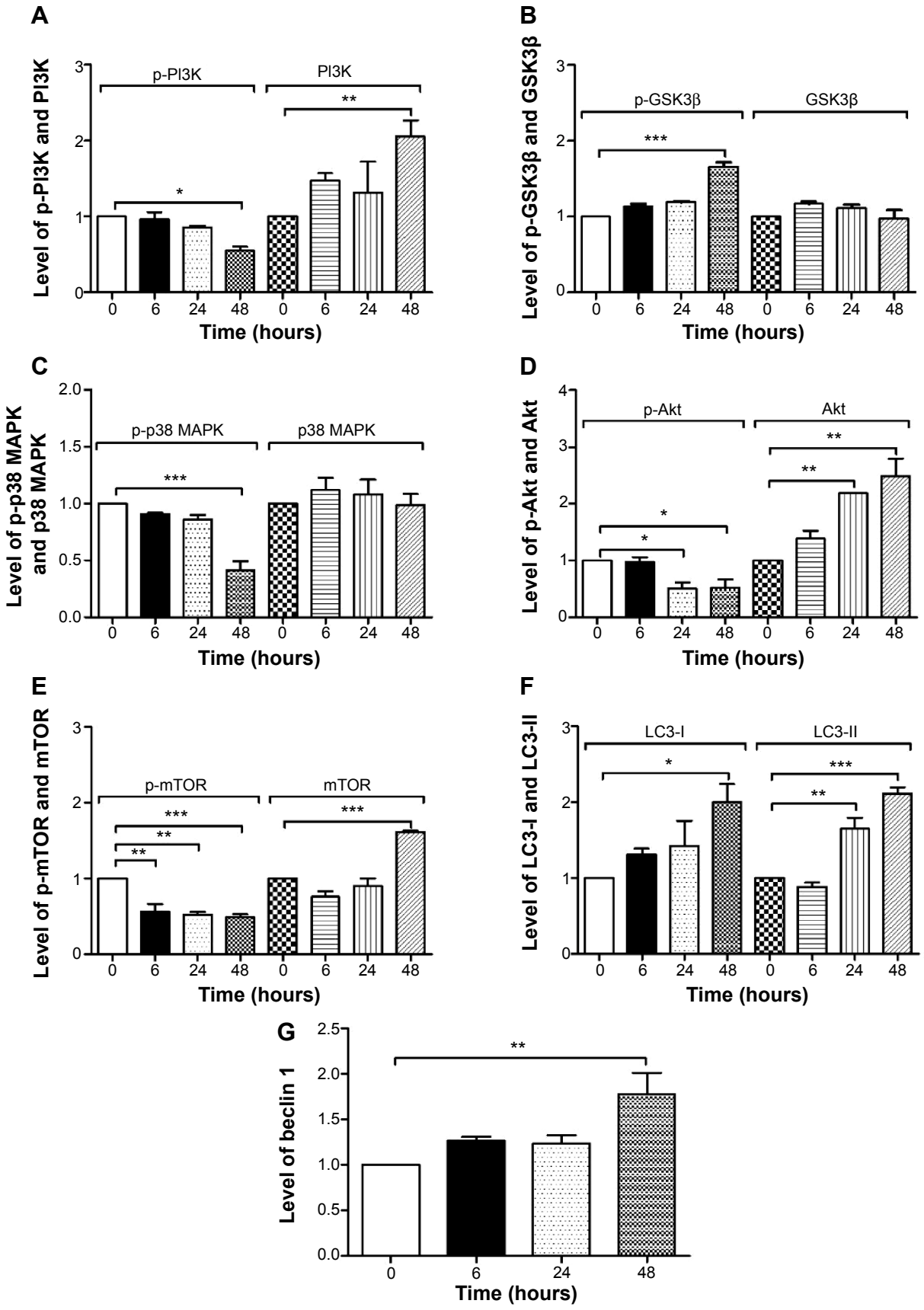

Figure 11 (*Continued*)

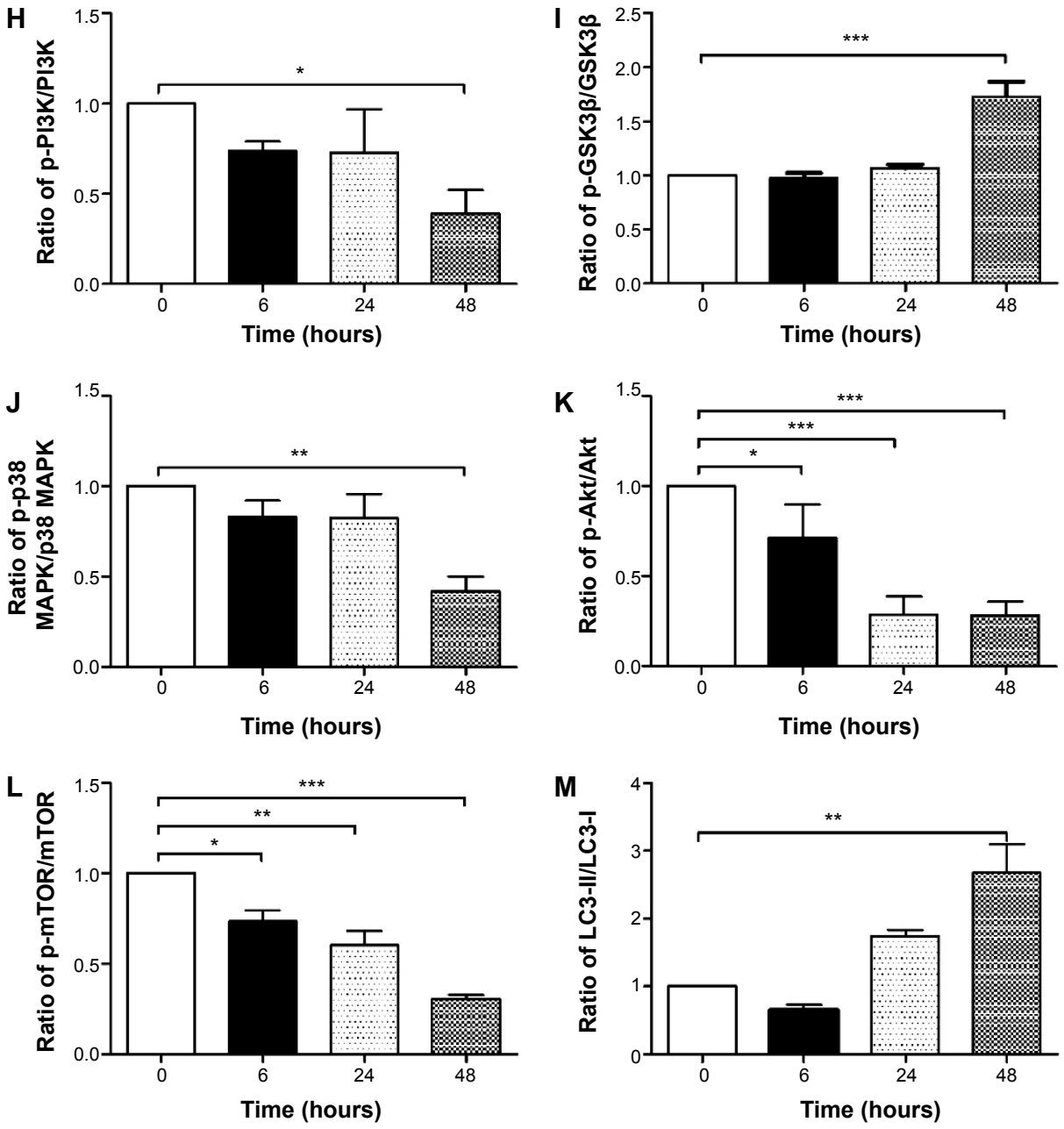

Figure 11 Effect of incubation time on the expression levels of autophagy-associated proteins in SCC25 cells treated with 5 μM PLB over 48 hours.

Notes: : (**A**) Bar graph shows the expression levels of p-PI3K and PI3K in SCC25 cells treated with PLB at 5 μM for 6, 24 and 48 hours; (**B**) bar graph shows the expression levels of p-GSK3β and GSK3β in SCC25 cells treated with PLB at 5 μM for 6, 24 and 48 hours; (**C**) bar graph shows the expression levels of p-p38 MAPK and p38 MAPK in SCC25 cells treated with PLB at 5 μM for 6, 24 and 48 hours; (**D**) bar graph shows the expression levels of p-Akt and Akt in SCC25 cells treated with PLB at 5 μM for 6, 24 and 48 hours; (**E**) bar graph shows the expression levels of p-mTOR and mTOR in SCC25 cells treated with PLB at 5 μM for 6, 24 and 48 hours; (**F**) bar graph shows the expression levels of LC3-I and LC3-II in SCC25 cells treated with PLB at 5 μM for 6, 24 and 48 hours; (**G**) bar graph shows the expression levels of beclin 1 in SCC25 cells treated with PLB at 5 μM for 6, 24 and 48 hours; (**H**) bar graph shows the ratio of p-pI3K over PI3K in SCC25 cells treated with PLB at 5 μM for 6, 24 and 48 hours; (**I**) bar graph shows the ratio of p-GSK3β over GSK3β in SCC25 cells treated with PLB at 5 μM for 6, 24 and 48 hours; (**J**) bar graph shows the ratio of p-p38 MAPK over p38 MAPK in SCC25 cells treated with PLB at 5 μM for 6, 24 and 48 hours; (**K**) bar graph shows the ratio of p-Akt over Akt in SCC25 cells treated with PLB at 5 μM for 6, 24 and 48 hours; (**L**) bar graph shows the ratio of p-mTOR over mTOR in SCC25 cells treated with PLB at 5 μM for 6, 24 and 48 hours; and (**M**) bar graph shows the ratio of LC3-II over LC3-I in SCC25 cells treated with PLB at 5 μM for 6, 24 and 48 hours. β-actin was used as the internal control. Data are the mean ± SD of three independent experiments. *$P<0.05$; **$P<0.01$; and ***$P<0.001$ by one-way ANOVA.

Abbreviations: ANOVA, analysis of variance; PLB, plumbagin; SD, standard deviation; Akt, protein kinase B; GSK3β, glycogen synthase kinase 3β; LC3, microtubule-associated protein 1 light chain 3; MAPK, mitogen-activated protein kinase; mTOR, mammalian target of rapamycin; PI3K, phosphatidylinositide 3 kinase.

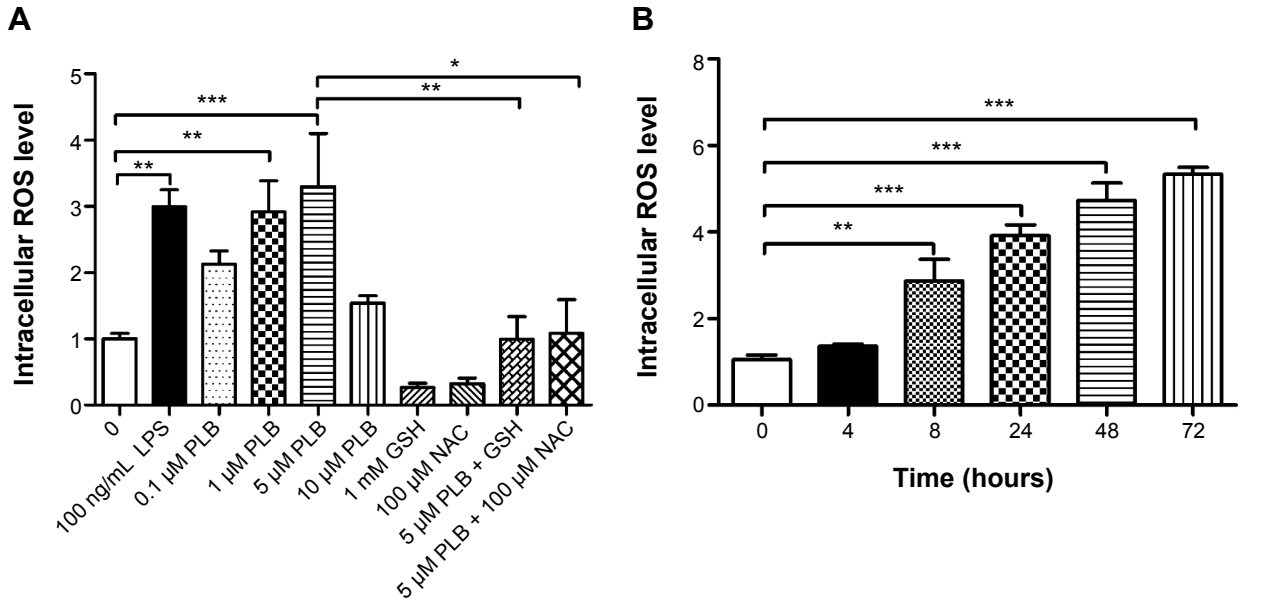

Figure 12 PLB induces the generation of cellular ROS in SCC25 cells.

Notes: (**A**) Bar graph shows the ROS generation level when the cells were treated with 0.1, 1, 5, and 10 μM PLB and 5 μM PLB +1 mM GSH or 5 μM PLB +100 μM NAC for 24 hours and (**B**) bar graph shows the ROS generation level when cells were treated with 5 μM PLB over 72 hours. LPS (100 ng/mL) was used as the positive control. Data are the mean ± SD of three independent experiments. *$P<0.05$; **$P<0.01$; and ***$P<0.001$ by one-way ANOVA.

Abbreviations: ANOVA, analysis of variance; GSH, L-glutathione; LPS, lipopolysaccharide; NAC, *N*-acetyl-L-cysteine; PLB, plumbagin; ROS, reactive oxygen species; SD, standard deviation.

PLB induces the generation of ROS in SCC25 cells

We next examined the effect of PLB on intracellular ROS generation in SCC25 cells. Briefly, cells were treated with PLB at 0.1, 1, 5, and 10 μM for 24 hours. LPS (100 ng/mL) was used as a positive control. The ROS production level was markedly increased by 2.9- and 3.3-fold when SCC25 cells were treated with 1 and 5 μM PLB for 24 hours, respectively, compared to the control cells ($P<0.01$ or 0.001; Figure 12A); there was no significant increase in ROS generation when treated with 10 μM PLB. Next, we tested the ROS generation-inducing effect of PLB in SCC25 cells over 72 hours. ROS production was significantly increased by 1.4-, 2.9-, 3.9-, 4.7-, and 5.3-fold when SCC25 cells were incubated with 5 μM PLB for 4, 8, 24, 48, and 72 hours, respectively, compared to the control cells ($P<0.01$ or 0.001; Figure 12B). Furthermore, GSH and NAC were used to verify the role of PLB in the promotion of intracellular ROS generation. The SCC25 cells were treated by 5 μM PLB with or without 1 mM GSH or 100 μM NAC. The PLB-induced generation of ROS was significantly attenuated by 55.0% and 46.0% when GSH or NAC were added, respectively, compared to PLB alone ($P<0.05$ or 0.01; Figure 12A). These results demonstrate that PLB induces the generation of cellular ROS in a concentration- and time-dependent manner in SCC25 cells.

Discussion

TSCC is the most common malignancy in oral cancers. TSCC is notorious for its lymphatic metastasis and relapse. Although comprehensive treatments are available that include radiotherapy, surgery, and chemotherapy, the therapeutic efficacy is not optimistic. This is partly due to hyperactive cell survival pathways and radiotherapy/chemotherapy resistance. Herein, it is urgent to probe into the corresponding molecule alterations and seek novel effective drugs for TSCC treatment. PLB is an active naphthoquinone constituent isolated from the roots of Plumbaginaceae plants. It is reported that PLB could exhibit anticancer activities in vitro and in vivo, which are due to its effects on multiple signaling pathways related to ROS generation, apoptosis, and autophagy.[23,46,47] In this study, we found that PLB induced cell apoptosis and autophagy via the PI3K/Akt/mTOR-mediated pathway and that p38 MAPK was also involved in the apoptosis- and autophagy-inducing effects of PLB in SCC25 cells. In addition, enhanced ROS generation was considered to contribute to these effects of PLB.

The pivotal mechanism by which tumor cells escape the cytotoxic effect of chemotherapeutic drugs is their protection from the induction and execution of apoptosis. Apoptosis can be mediated by the caspase family of cysteine proteases, which can be triggered by the intrinsic mitochondria/cytochrome-mediated pathway and the extrinsic death

receptor pathway.[8,48] The two pathways both lead to the activation of caspases 3, 6, and 7. In the extrinsic pathway, various stimuli such as tumor necrosis factor receptor can bind to the extracellular death ligands, which could induce the activation of caspase 8 and later caspases 3 and 7. All these processes will lead to cell death eventually.[8,48] In the intrinsic pathway, cytochrome c is released into the cytoplasm, which will form a multiprotein complex called 'apoptosome', and induce the activation of the caspase cascade.[49] The pro-apoptotic effect of PLB has been studied in multiple cancer cell lines, including breast cancer, non-small-cell lung carcinoma (NSCLC), melanoma, and leukemia.[25,50–52] In the present study, we observed that PLB can induce apoptosis in SCC25 cells in a concentration- and time-dependent manner. It is known that mitochondrial disruption and the subsequent release of cytochrome c initiates the process of apoptosis.[8] The Bcl-2 gene family encodes proteins that control apoptotic signaling. According to its role in apoptosis, the Bcl-2 family can be classified into two subtypes: pro-apoptotic members (eg, Bax and Bak) and anti-apoptotic members (eg, Bcl-2 and Bcl-xl). The balance of the Bcl-2 family determines the release of cytochrome c as well as subsequent activation of the caspase cascade. Anti-apoptotic members of Bcl-2 family can be sequestered by post-translational modification and/or by boosted expression of PUMA, which is a critical regulator of p53-mediated cell apoptosis.[8] In our study, we found that the expression level of PUMA was significantly increased after PLB treatment. The cytosolic level of cytochrome c was also greatly increased, followed by activation of caspase 9 and caspase 3. The activated caspase 3 eventually induced apoptosis with increased Bax and decreased Bcl-2, both in a concentration- and time-dependent manner. The results demonstrate that PLB initiates mitochondria-dependent apoptosis in SCC25 cells with the involvement of p53.

Autophagy (also known as caspase-independent form of or type 2 programmed cell death) is a physiological and evolutionarily conserved process maintaining cellular homeostasis and genomic integrity by engulfing and degrading malfunctioning organelles and proteins in living cells. It is suggested that the basal level of autophagy is beneficial for cell survival.[4] This complicated process can be briefly divided into several steps, including initiation, vesicle elongation, maturation, docking and fusion, and vesicle breakdown, and degradation.[4] The double membrane enclosed vesicles in the cytoplasm are the most prominent morphological change observed in autophagy. These vesicles fuse with lysosomes and deliver their cargo for degradation by lysosomal enzymes.[5] The PI3K/Akt/mTOR signaling pathway is an important signaling cascade regulating cell survival, proliferation, growth, differentiation, metabolism, migration, and angiogenesis.[53,54] Normally, this pathway is initiated upon binding of a growth factor to a receptor tyrosine kinase.[55] PI3K activates the serine/threonine kinase Akt, which in turn phosphorylates and activates the serine/threonine kinase mTOR through a cascade of regulators.[56] Currently, targeting apoptosis and autophagy has been put forward as a potential strategy in cancer treatment.[51,57] In our study, PLB induced autophagy in SCC25 cells, which may partly contribute to its anticancer activity. Of note, our previous study has revealed that PLB predominantly induced autophagy rather than apoptosis, through inhibition of the PI3K/Akt/mTOR pathway in NSCLC cells.[24] In the present study, we also observed that PLB induced more autophagy than apoptosis, especially at the concentration of 1 μM. Moreover, PLB can significantly induce autophagy after 8 hours of treatment. PLB exerts its autophagy-inducing effect via inhibition of the PI3K/Akt/mTOR signaling pathway in SCC25 cells. Although the role of autophagy in cancer is paradoxical, as it can function as a tumor suppressor at the early stage of tumor development, it can also be used as a cytoprotection mechanism to promote survival in established tumors.[6,58]

GSK3 is a serine/threonine protein kinase that binds the phosphate molecules to serine and threonine amino acid residues. In mammals, there are two types of GSK3, including GSK3α and GSK3β. GSK3β is the most researched GSK3, as it is involved in Alzheimer's disease, diabetes mellitus type 2, inflammation, and cancer.[59–63] Recent studies suggest that GSK3β is involved in cellular apoptosis and autophagy.[64–68] The active form of GSK3β is in the dephosphorylated state; when it is phosphorylated, GSK3β loses its activity. We found that PLB could enhance the phospharylation level of GSK3β which may contribute to the inhibition of mTOR. Of note, the inhibition level of GSK3β in the separate concentration and time course experiments has a minor discrepancy; this may be due to different SCC25 passages and different batches. Furthermore, PLB significantly suppressed the phosphorylation of p38 MAPK. p38 MAPK is a key signaling pathway controlling cell growth, proliferation, and cell survival in various cancer types.[34,69] p38 MAPK is responsive to multiple stress stimuli, such as heat shock, cytokines, and osmotic shock, and regulates cell differentiation, apoptosis, and autophagy.[6,8] We employed SB202190, which is a p38 MAPK inhibitor, to examine the levels of PLB-induced autophagy. The results showed a remarkable increase in autophagic cell death. Taken

together, GSK3β and p38 MAPK play an important role in PLB-induced autophagy in TSCC cells.

Several studies have shown that PLB could increase intracellular ROS levels, and thus contribute to the cell death observed in various cancer cell lines.[24,25,70] In this study, we found a significant inducing effect of PLB on ROS generation in SCC25 cells. The quinone core of PLB can transfer electrons in the mitochondria respiratory pathways.[11] After employing GSH and NAC, which are both ROS scavengers, PLB-induced ROS was significantly attenuated. The ROS-inducing effect of PLB has been verified in our study. However, we did not investigate the source of the ROS. NADPH oxidase is the major intracellular enzymatic source of ROS, which could be a potential target of PLB. In our next experiment, we plan to further explore the source of PLB-induced ROS.

In addition, we have observed that PLB induced both apoptosis and autophagy in SCC25 cells, and that PLB can induce autophagy at a lower concentration and over a shorter time period. We predict that autophagy may be much more important in PLB-mediated anticancer events. However, we should further verify it by using an autophagy inhibitor to test the apoptosis level and vice versa. The crosstalk between apoptosis and autophagy is very complicated, with multiple signaling pathways involved. We cannot make conclusions hastily without considering the specific cancer cell types and the tumor microenvironment. Under certain physiological conditions, autophagy has cytoprotective effects and negatively regulates apoptosis and vice versa. At the subcellular level, the mitochondria play a critical role in the processes of apoptosis, autophagy, and ROS generation. Various stimuli from the outer membranes can directly influence the function of mitochondria. Loss of mitochondrial membrane potential can easily lead to the release of pro-apoptotic molecules, which eventually initiate the execution of apoptosis. However, autophagy can, to some extent, dispose of dysfunctional mitochondria via lysosome-mediated degradation. ROS can be generated through uncontrolled electron delivery or deficiency in ROS scavengers such as GSH. Considering all these, we speculate that apoptosis and autophagy induced by PLB can be coordinated by some important molecules, including ROS, GSK3β, p53, beclin 1, and Akt. Under certain conditions, PLB can mediate apoptosis and autophagy in a harmonious manner to achieve its anticancer properties. PLB shows great potential in cancer therapy, targeting both apoptosis and autophagy via multiple signaling pathways such as PI3K/Akt/mTOR, p38 MAPK, GSK3β, p53, and ROS-associated pathways.

In summary, we discussed the potential molecular mechanisms of PLB for its anticancer effect on human TSCC SCC25 cells. The effect of PLB was attributed to ROS generation, mitochondrial function, apoptosis, and autophagy, as well as regulation of their associated signaling pathways. PLB increased the intracellular levels of ROS, activated the mitochondria-dependent apoptotic pathway, and induced autophagy in TSCC SCC25 cells. The inhibition of PI3K/Akt/mTOR, p38 MAPK, and GSK3β signaling pathways and promotion of ROS generation by PLB can finally contribute to its anticancer activity. PLB may represent a new anticancer drug that can kill TSCC cells. Although, we did not examine the crosstalk of apoptosis and autophagy and the ROS source in this study, we provided some valuable information for the potential role of PLB in TSCC treatment for the first time. However, more conclusive evidence is needed to support this. For our next project, we plan to investigate the relationship between apoptosis and autophagy and other possible signals mediating the effect of PLB on TSCC cells.

Acknowledgment

The authors appreciate the financial support by the Science and Technology Support Program (Grant no 20142BBG70060), Department of Science and Technology, Nanchang, Jiangxi Province, People's Republic of China.

Disclosure

The authors report no conflicts of interest in this work.

References

1. Siegel R, Ma J, Zou Z, Jemal A. Cancer statistics, 2014. *CA Cancer J Clin*. 2014;64(1):9–29.
2. Markopoulos AK. Current aspects on oral squamous cell carcinoma. *Open Dent J*. 2012;6:126–130.
3. Dogan E, Cetinayak HO, Sarioglu S, Erdag TK, Ikiz AO. Patterns of cervical lymph node metastases in oral tongue squamous cell carcinoma: implications for elective and therapeutic neck dissection. *J Laryngol Otol*. 2014;128(3):268–273.
4. Choi AM, Ryter SW, Levine B. Autophagy in human health and disease. *N Engl J Med*. 2013;368(19):1845–1846.
5. Choi KS. Autophagy and cancer. *Exp Mol Med*. 2012;44(2):109–120.
6. Denton D, Nicolson S, Kumar S. Cell death by autophagy: facts and apparent artefacts. *Cell Death Differ*. 2012;19(1):87–95.
7. Fuchs Y, Steller H. Programmed cell death in animal development and disease. *Cell*. 2011;147(4):742–758.
8. Taylor RC, Cullen SP, Martin SJ. Apoptosis: controlled demolition at the cellular level. *Nat Rev Mol Cell Biol*. 2008;9(3):231–241.
9. Green DR. Apoptotic pathways: ten minutes to dead. *Cell*. 2005;121(5):671–674.
10. Kurokawa M, Kornbluth S. Caspases and kinases in a death grip. *Cell*. 2009;138(5):838–854.
11. Padhye S, Dandawate P, Yusufi M, Ahmad A, Sarkar FH. Perspectives on medicinal properties of plumbagin and its analogs. *Med Res Rev*. 2012;32(6):1131–1158.

12. Sung B, Oyajobi B, Aggarwal BB. Plumbagin inhibits osteoclastogenesis and reduces human breast cancer-induced osteolytic bone metastasis in mice through suppression of RANKL signaling. *Mol Cancer Ther*. 2012; 11(2):350–359.
13. Mishra BB, Singh DD, Kishore N, Tiwari VK, Tripathi V. Antifungal constituents isolated from the seeds of *Aegle marmelos*. *Phytochemistry*. 2010;71(2–3):230–234.
14. Kuete V, Alibert-Franco S, Eyong KO, et al. Antibacterial activity of some natural products against bacteria expressing a multidrug-resistant phenotype. *Int J Antimicrob Agents*. 2011;37(2):156–161.
15. Pradeepa V, Sathish-Narayanan S, Kirubakaran SA, Senthil-Nathan S. Antimalarial efficacy of dynamic compound of plumbagin chemical constituent from *Plumbago zeylanica* Linn (Plumbaginaceae) against the malarial vector *Anopheles stephensi* Liston (Diptera: Culicidae). *Parasitol Res*. 2014;113(8):3105–3109.
16. Checker R, Patwardhan RS, Sharma D, et al. Plumbagin, a vitamin K_3 analogue, abrogates lipopolysaccharide-induced oxidative stress, inflammation and endotoxic shock via NF-κB suppression. *Inflammation*. 2014;37(2):542–554.
17. Sharma I, Gusain D, Dixit VP. Hypolipidaemic and antiatherosclerotic effects of plumbagin in rabbits. *Indian J Physiol Pharmacol*. 1991;35(1): 10–14.
18. Zhang K, Ge Z, Da Y, et al. Plumbagin suppresses dendritic cell functions and alleviates experimental autoimmune encephalomyelitis. *J Neuroimmunol*. 2014;273(1–2):42–52.
19. Sinha S, Pal K, Elkhanany A. Plumbagin inhibits tumorigenesis and angiogenesis of ovarian cancer cells in vivo. *Int J Cancer*. 2013;132(5): 1201–1212.
20. Qiu JX, He YQ, Wang Y. Plumbagin induces the apoptosis of human tongue carcinoma cells through the mitochondria-mediated pathway. *Med Sci Monit Basic Res*. 2013;19:228–236.
21. Xu TP, Shen H, Liu LX, Shu YQ. Plumbagin from *Plumbago zeylanica* L induces apoptosis in human non-small cell lung cancer cell lines through NF-κB inactivation. *Asian Pac J Cancer Prev*. 2013;14(4): 2325–2331.
22. Hsu YL, Cho CY, Kuo PL, Huang YT, Lin CC. Plumbagin (5-hydroxy-2-methyl-1,4-naphthoquinone) induces apoptosis and cell cycle arrest in A549 cells through p53 accumulation via c-Jun NH_2-terminal kinase-mediated phosphorylation at serine 15 in vitro and in vivo. *J Pharmacol Exp Ther*. 2006;318(2):484–494.
23. Kuo P, Hsu YL, Cho CY. Plumbagin induces G_2-M arrest and autophagy by inhibiting the AKT/mammalian target of rapamycin pathway in breast cancer cells. *Mol Cancer Ther*. 2006;5(12):3209–3221.
24. Li YC, He SM, He ZX, et al. Plumbagin induces apoptotic and autophagic cell death through inhibition of the PI3K/Akt/mTOR pathway in human non-small cell lung cancer cells. *Cancer Lett*. 2014; 344(2):239–259.
25. Sun J, McKallip RJ. Plumbagin treatment leads to apoptosis in human K562 leukemia cells through increased ROS and elevated TRAIL receptor expression. *Leuk Res*. 2011;35(10):1402–1408.
26. Kumar S, Gautam S, Sharma A. Antimutagenic and antioxidant properties of plumbagin and other naphthoquinones. *Mutat Res*. 2013; 755(1):30–41.
27. Ma S, Li Q, Pan F. CXCR4 promotes GSK3β expression in pancreatic cancer cells via the Akt pathway. *Int J Clin Oncol*. Epub 2014 Aug 23.
28. Kao SH, Wang WL, Chen CY, et al. GSK3β controls epithelial-mesenchymal transition and tumor metastasis by CHIP-mediated degradation of Slug. *Oncogene*. 2014;33(24):3172–3182.
29. Zeng J, Liu D, Qiu Z, et al. GSK3β overexpression indicates poor prognosis and its inhibition reduces cell proliferation and survival of non-small cell lung cancer cells. *PLoS One*. 2014;9(3):e91231.
30. Zhang JS, Herreros-Villanueva M, Koenig A, et al. Differential activity of GSK-3 isoforms regulates NF-κB and TRAIL- or TNFα induced apoptosis in pancreatic cancer cells. *Cell Death Dis*. 2014;5:e1142.
31. Gavilán E, Sánchez-Aguayo I, Daza P, Ruano D. GSK-3β signaling determines autophagy activation in the breast tumor cell line MCF7 and inclusion formation in the non-tumor cell line MCF10A in response to proteasome inhibition. *Cell Death Dis*. 2013;4:e572.
32. Han J, Lee JD, Bibbs L, Ulevitch RJ. A MAP kinase targeted by endotoxin and hyperosmolarity in mammalian cells. *Science*. 1994; 265(5173):808–811.
33. Ono K, Han J. The p38 signal transduction pathway: activation and function. *Cell Signal*. 2000;12(1):1–13.
34. Sui X, Kong N, Ye L, et al. p38 and JNK MAPK pathways control the balance of apoptosis and autophagy in response to chemotherapeutic agents. *Cancer Lett*. 2014;344(2):174–179.
35. Zhou CH, Pan J, Huang H, et al. Salusin-β, but not salusin-α, promotes human umbilical vein endothelial cell inflammation via the p38 MAPK/JNK-NF-κB Pathway. *PLoS One*. 2014;9(9):e107555.
36. Kobayashi M, Takeyoshi I, Yoshinari D, Matsumoto K, Morishita Y. P38 mitogen-activated protein kinase inhibition attenuates ischemia-reperfusion injury of the rat liver. *Surgery*. 2002;131(3): 344–349.
37. Yang DP, Kim J, Syed N, et al. p38 MAPK activation promotes denervated Schwann cell phenotype and functions as a negative regulator of Schwann cell differentiation and myelination. *J Neurosci*. 2012; 32(21): 7158–7168.
38. Leelahavanichkul K, Amornphimoltham P, Molinolo AA, Basile JR, Koontongkaew S, Gutkind JS. A role for p38 MAPK in head and neck cancer cell growth and tumor-induced angiogenesis and lymphangiogenesis. *Mol Oncol*. 2014;8(1):105–118.
39. Arthur JS, Ley SC. Mitogen-activated protein kinases in innate immunity. *Nat Rev Immunol*. 2013;13(9):679–692.
40. Koul HK, Pal M, Koul S. Role of p38 MAP kinase signal transduction in solid tumors. *Genes Cancer*. 2013;4(9–10):342–359.
41. Zhang X, Tang N, Hadden TJ, Rishi AK. Akt, FoxO and regulation of apoptosis. *Biochim Biophys Acta*. 2011;1813(11):1978–1986.
42. Rabinowitz JD, White E. Autophagy and metabolism. *Science*. 2010;330(6009):1344–1348.
43. Kang R, Zeh HJ, Lotze MT, Tang D. The Beclin 1 network regulates autophagy and apoptosis. *Cell Death Differ*. 2011;18(4):571–580.
44. Maiuri MC, Criollo A, Kroemer G. Crosstalk between apoptosis and autophagy within the Beclin 1 interactome. *EMBO J*. 2010;29(3): 515–516.
45. Kabeya Y, Mizushima N, Ueno T, et al. LC3, a mammalian homologue of yeast Apg8p, is localized in autophagosome membranes after processing. *EMBO J*. 2000;19(21):5720–5728.
46. Aziz MH, Dreckschmidt NE, Verma AK. Plumbagin, a medicinal plant-derived naphthoquinone, is a novel inhibitor of the growth and invasion of hormone-refractory prostate cancer. *Cancer Res*. 2008;68(21): 9024–9032.
47. Wang CC, Chiang YM, Sung SC, Hsu YL, Chang JK, Kuo PL. Plumbagin induces cell cycle arrest and apoptosis through reactive oxygen species/c-Jun N-terminal kinase pathways in human melanoma A375.S2 cells. *Cancer Lett*. 2008;259(1):82–98.
48. Estaquier J, Vallette F, Vayssiere JL, Mignotte B. The mitochondrial pathways of apoptosis. *Adv Exp Med Biol*. 2012;942:157–183.
49. Richter-Larrea JA, Robles EF, Fresquet V, et al. Reversion of epigenetically mediated BIM silencing overcomes chemoresistance in Burkitt lymphoma. *Blood*. 2010;116(14):2531–2542.
50. Ahmad A, Banerjee S, Wang Z, Kong D, Sarkar FH. Plumbagin-induced apoptosis of human breast cancer cells is mediated by inactivation of NF-κB and Bcl-2. *J Cell Biochem*. 2008;105(6):1461–1471.
51. Ding YH, Zhou ZW, Ha CF, et al. The Aurora kinase A inhibitor alisertib induces apoptosis and autophagy but inhibits epithelial to mesenchymal transition in human epithelial ovarian cancer cells. *Drug Des Devel Ther*. 2015;9:425–464.
52. Pennington K, Pulaski H, Pennington M, Liu JR. Too much of a good thing: suicide prevention promotes chemoresistance in ovarian carcinoma. *Curr Cancer Drug Targets*. 2010;10(6):575–583.
53. Guertin DA, Sabatini DM. Defining the role of mTOR in cancer. *Cancer Cell*. 2007;12(1):9–22.
54. Slomovitz BM, Coleman RL. The PI3K/AKT/mTOR pathway as a therapeutic target in endometrial cancer. *Clin Cancer Res*. 2012;18(21): 5856–5864.

55. Wozney JL, Antonarakis ES. Growth factor and signaling pathways and their relevance to prostate cancer therapeutics. *Cancer Metastasis Rev*. 2014;33(2–3):581–594.
56. Rodon J, Dienstmann R, Serra V, Tabernero J. Development of PI3K inhibitors: lessons learned from early clinical trials. *Nat Rev Clin Oncol*. 2013;10(3):143–153.
57. Zielinski RR, Eigl BJ, Chi KN. Targeting the apoptosis pathway in prostate cancer. *Cancer J*. 2013;19(1):79–89.
58. Klionsky DJ, Emr SD. Autophagy as a regulated pathway of cellular degradation. *Science*. 2000;290(5497):1717–1721.
59. Piazza F, Manni S, Semenzato G. Novel players in multiple myeloma pathogenesis: role of protein kinases CK2 and GSK3. *Leuk Res*. 2013; 37(2):221–227.
60. Kim TW, Michniewicz M, Bergmann DC, Wang ZY. Brassinosteroid regulates stomatal development by GSK3-mediated inhibition of a MAPK pathway. *Nature*. 2012;482(7385):419–422.
61. Gao C, Hölscher C, Liu Y, Li L. GSK3: a key target for the development of novel treatments for type 2 diabetes mellitus and Alzheimer disease. *Rev Neurosci*. 2012;23(1):1–11.
62. Jope RS, Yuskaitis CJ, Beurel E. Glycogen synthase kinase-3 (GSK3): inflammation, diseases, and therapeutics. *Neurochem Res*. 2007; 32(4–5):577–595.
63. Hernandez F, Lucas JJ, Avila J. GSK3 and tau: two convergence points in Alzheimer's disease. *J Alzheimers Dis*. 2013;33 (Suppl 1):S141–S144.
64. Zimmermann C, Santos A, Gable K, et al. TORC1 inhibits GSK3-mediated Elo2 phosphorylation to regulate very long chain fatty acid synthesis and autophagy. *Cell Rep*. 2013;5(4):1036–1046.
65. Niu S, Yuan D, Jiang X, Che Y. 11′-Deoxyverticillin A (C42) promotes autophagy through K-Ras/GSK3 signaling pathway in HCT116 cells. *Protein Cell*. 2014;5(12):945–949.
66. Lin SY, Li TY, Liu Q, et al. GSK3-TIP60-ULK1 signaling pathway links growth factor deprivation to autophagy. *Science*. 2012;336(6080):477–481.
67. Kurosu T, Nagao T, Wu N, Oshikawa G, Miura O. Inhibition of the PI3K/Akt/GSK3 pathway downstream of BCR/ABL, Jak2-V617F, or FLT3-ITD downregulates DNA damage-induced Chk1 activation as well as G_2/M arrest and prominently enhances induction of apoptosis. *PLoS One*. 2013;8(11):e79478.
68. Rahmani M, Aust MM, Attkisson E, Williams DC Jr, Ferreira-Gonzalez A, Grant S. Dual inhibition of Bcl-2 and Bcl-xL strikingly enhances PI3K inhibition-induced apoptosis in human myeloid leukemia cells through a GSK3- and Bim-dependent mechanism. *Cancer Res*. 2013;73(4): 1340–1351.
69. Yang J, He J, Wang J, et al. Constitutive activation of p38 MAPK in tumor cells contributes to osteolytic bone lesions in multiple myeloma. *Leukemia*. 2012;26(9):2114–2123.
70. Xu KH, Lu DP. Plumbagin induces ROS-mediated apoptosis in human promyelocytic leukemia cells in vivo. *Leuk Res*. 2010;34(5):658–665.